Topology of light polarization vortices in photonic crystals

Grazia Salerno — University of Pisa

Topology and Disorder in Wave Physics — 20th November 2025 — Cargèse

Outline

- *Photonic crystals bands and guided resonances*
- *A type of topological state in photonic crystals: bound states in the continuum*
- *Non-Hermitian topology in the far field and bulk-radiation correspondence*
- *Loss-designed lasing in bound states in the continuum*

Photonic crystals

From Maxwell's equations to an eigenvalue equation for Bloch modes

$$\nabla \times \nabla \times \mathbf{E} = \frac{\epsilon(\mathbf{r})}{c^2} \frac{\partial \mathbf{E}}{\partial^2 t}$$

$$\mathbf{E}(\mathbf{r}, t) = \mathbf{E}(\mathbf{r}) e^{-i\omega t}$$

$$\mathbf{E}(\mathbf{r}) = \sum_{\mathbf{G}} e^{i(\mathbf{k}+\mathbf{G})\cdot\mathbf{r}} \psi_{\mathbf{G}}(\mathbf{k}) |\mathbf{p}_{\mathbf{G}}\rangle$$

$\mathbf{k}$ is the in-plane wavevector
$\mathbf{G}$ is the reciprocal lattice vector
$\mathbf{p}_{\mathbf{G}}$ is the polarization vector

$$\mathbf{p}_{\mathbf{G}}(\mathbf{k}) \cdot (\mathbf{k} + \mathbf{G}) = 0$$

Bloch's theorem applies $\epsilon(\mathbf{r}) = \epsilon(\mathbf{r} + \mathbf{R})$

$$\epsilon(\mathbf{r}) = \sum_{\mathbf{G}} \epsilon_{\mathbf{G}} e^{i\mathbf{G}\cdot\mathbf{r}}$$

Generalized eigenvalue problem

$$(\mathbf{k} + \mathbf{G}) \cdot (\mathbf{k} + \mathbf{G}) \psi_{\mathbf{G}}(\mathbf{k}) |\mathbf{p}_{\mathbf{G}}(\mathbf{k})\rangle = \frac{\omega^2}{c^2} \epsilon_{\mathbf{G}-\mathbf{G}'} \psi_{\mathbf{G}'}(\mathbf{k}) |\mathbf{p}_{\mathbf{G}'}(\mathbf{k})\rangle$$

Periodic modulation of refractive index creates band structures for photons

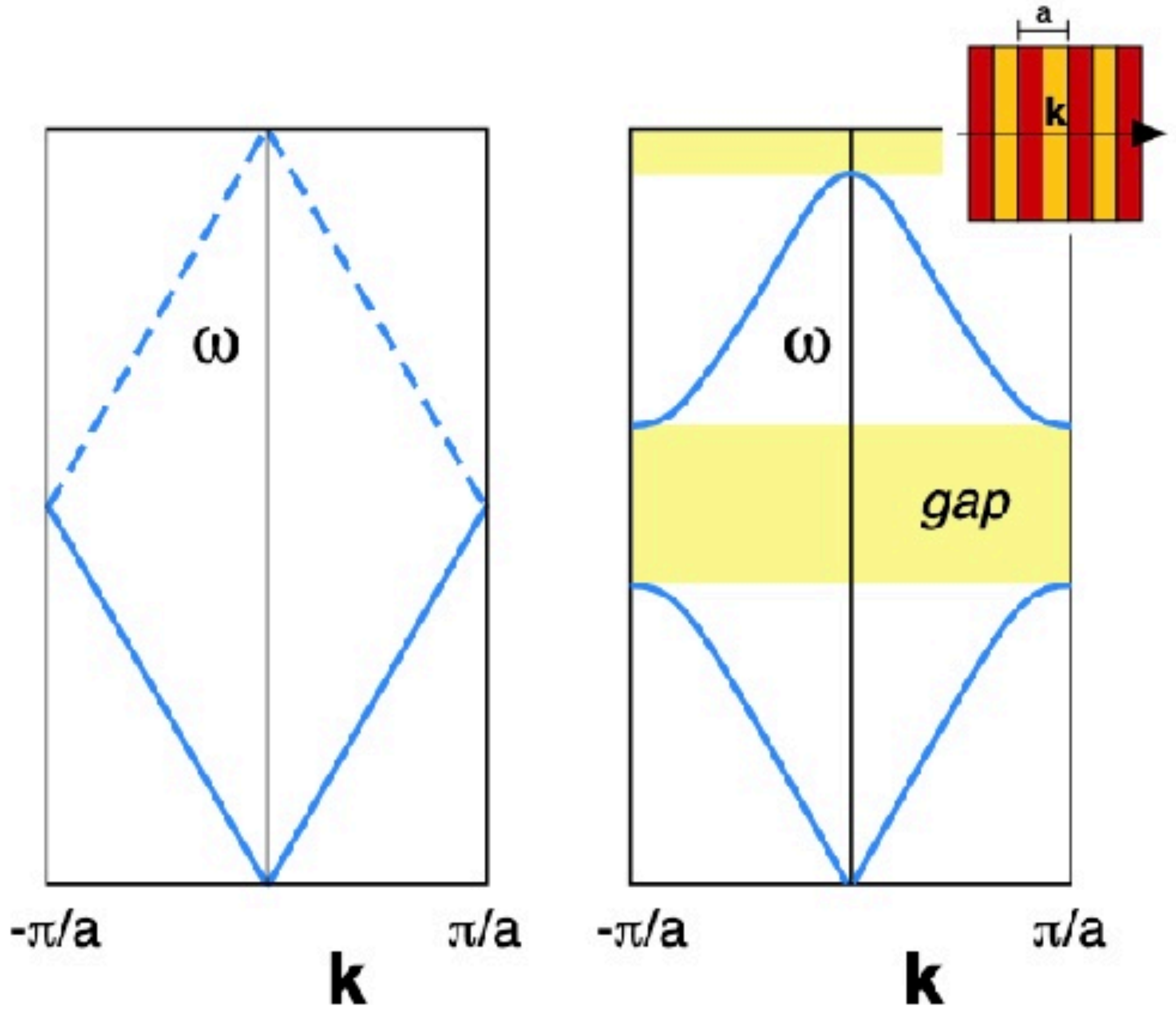

Photonic Crystals - Molding the Flow of Light by Joannopoulos, Johnson, Winn, Meade

Guided resonances and BICs

Radiation to the continuum and symmetry-protected modes

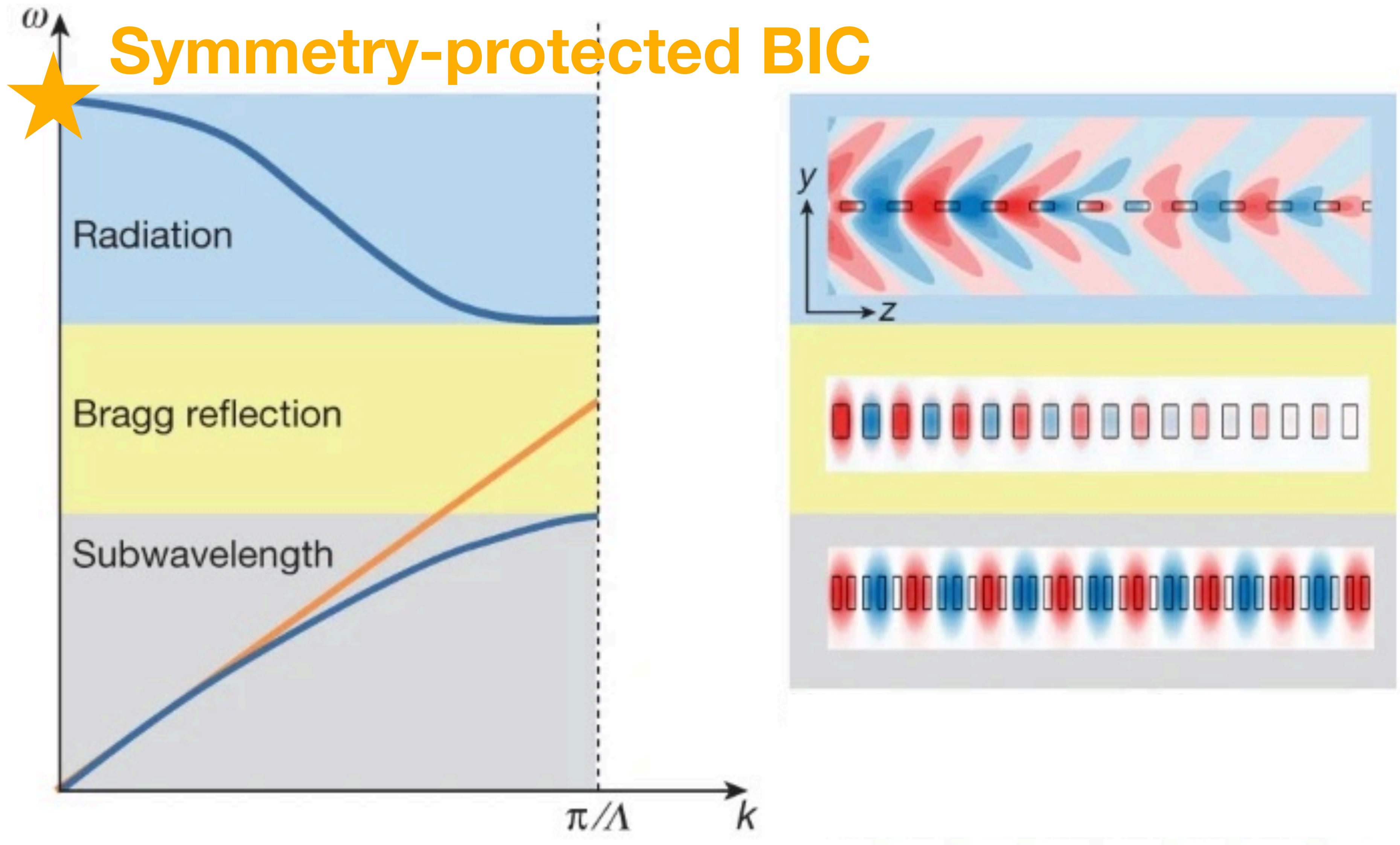

- Bound states in the continuum (BICs) are *embedded eigenvalues,* decoupled from the continuum spectrum

- General phenomena of waves (electromagnetic, acoustic, mechanical, water/elastic, quantum)

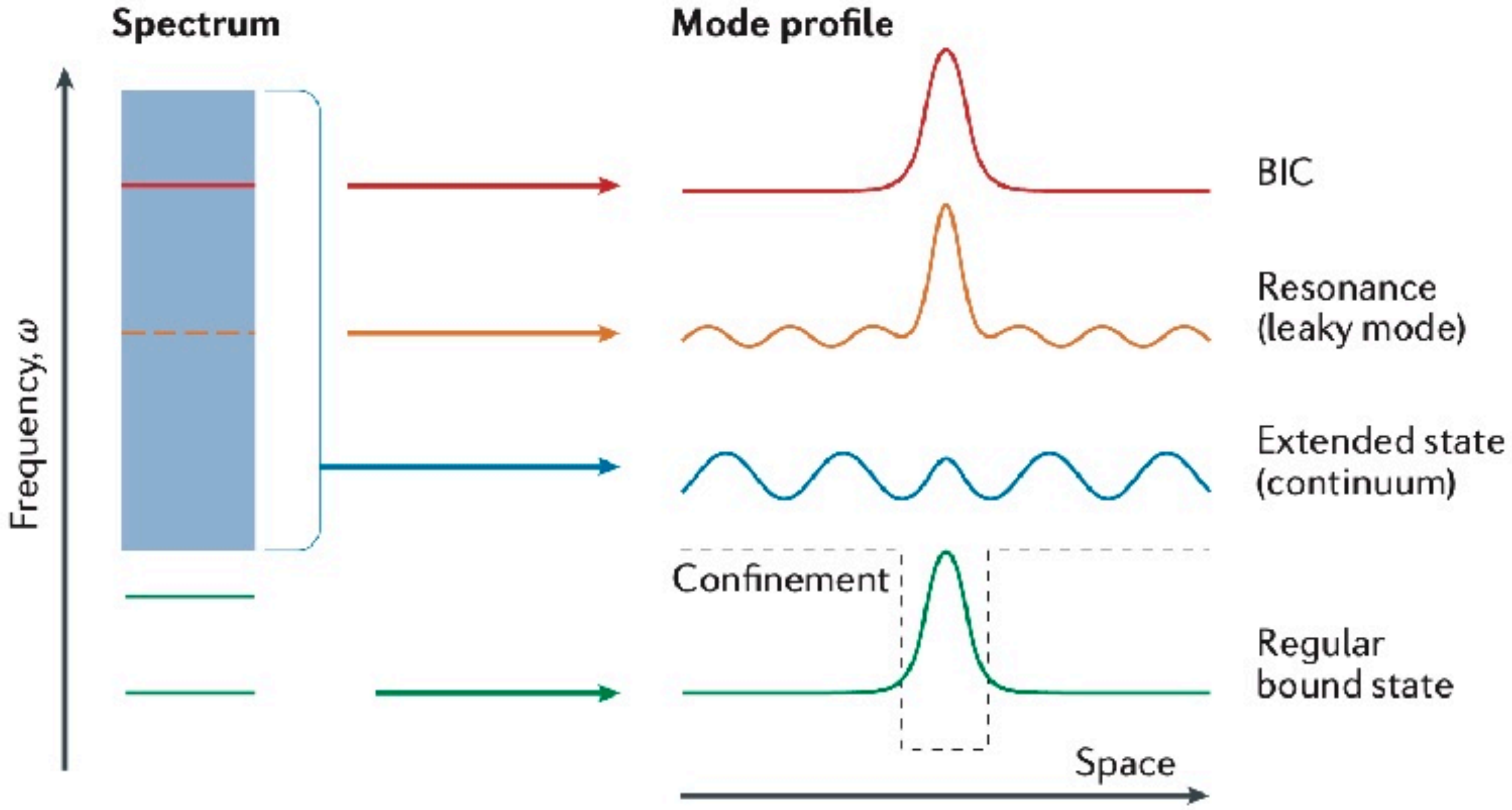

Hsu *et al. Nat. Rev. Mater.* **1,** 16048 (2016)

Cheben *et al. Nature* **560,** 565 (2018)

Topological origin of BICs

Light polarization vortices

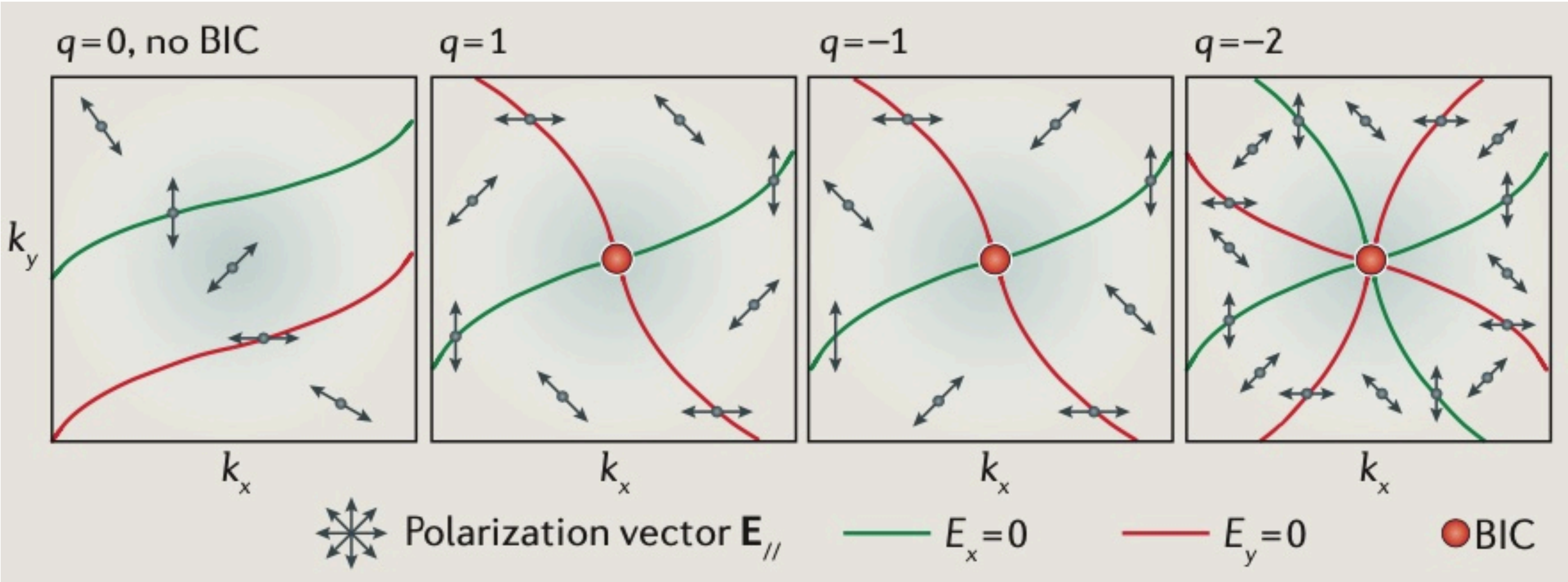

Radiation channels destructively interfere in the far-field.
Occur at high-symmetry-point in Brillouin zone.

Bound states in the continuum cannot radiate because **there is no way to assign a far-field polarization** that is consistent with neighbouring k points.

Bound states in the continuum are only possible when there is vorticity in the polarization field, protected by the existence of a non-trivial topological charge (winding):

$$q = \frac{1}{2\pi} \int \mathrm{d}\mathbf{k} \cdot \nabla_{\mathbf{k}} \phi(\mathbf{k})$$

Zhen *et al., Phys. Rev. Lett.* **113**, 257401 (2014)

Symmetry protection of BICs

Group theory and irreducible representation

Symmetry	IR	$\arg(\epsilon_{\mathrm{IR}})$	q
C_4	A	0	$+1$
	B	π	-1
	E^*	$\pi/2$	0

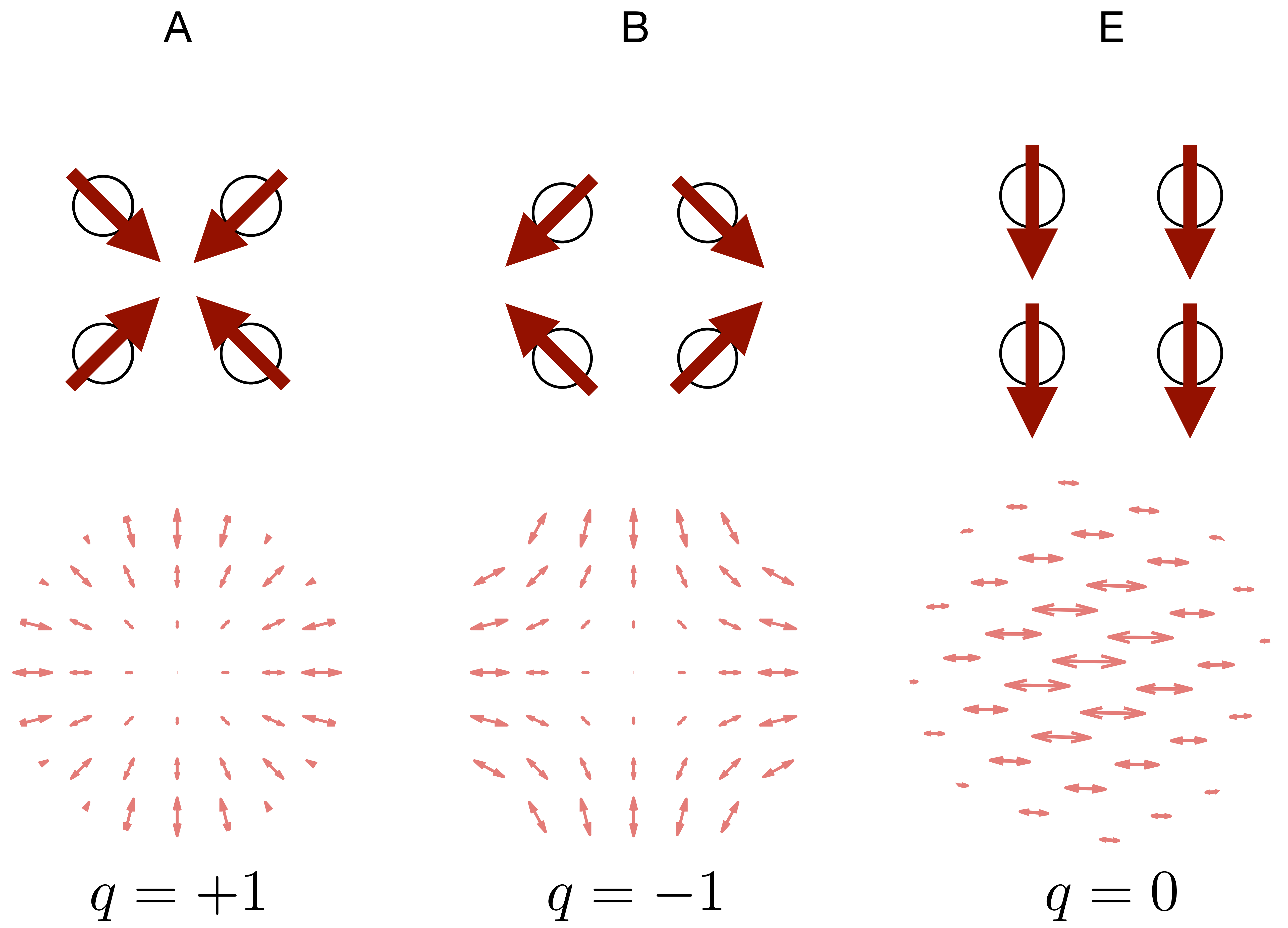

Symmetry protection of BICs

Group theory and irreducible representation

Symmetry	IR	$\arg(\epsilon_{\mathrm{IR}})$	q
C_6	A	0	$+1$
	B	π	-2
	E_1^*	$\pi/3$	0
	E_2^*	$2\pi/3$	-1

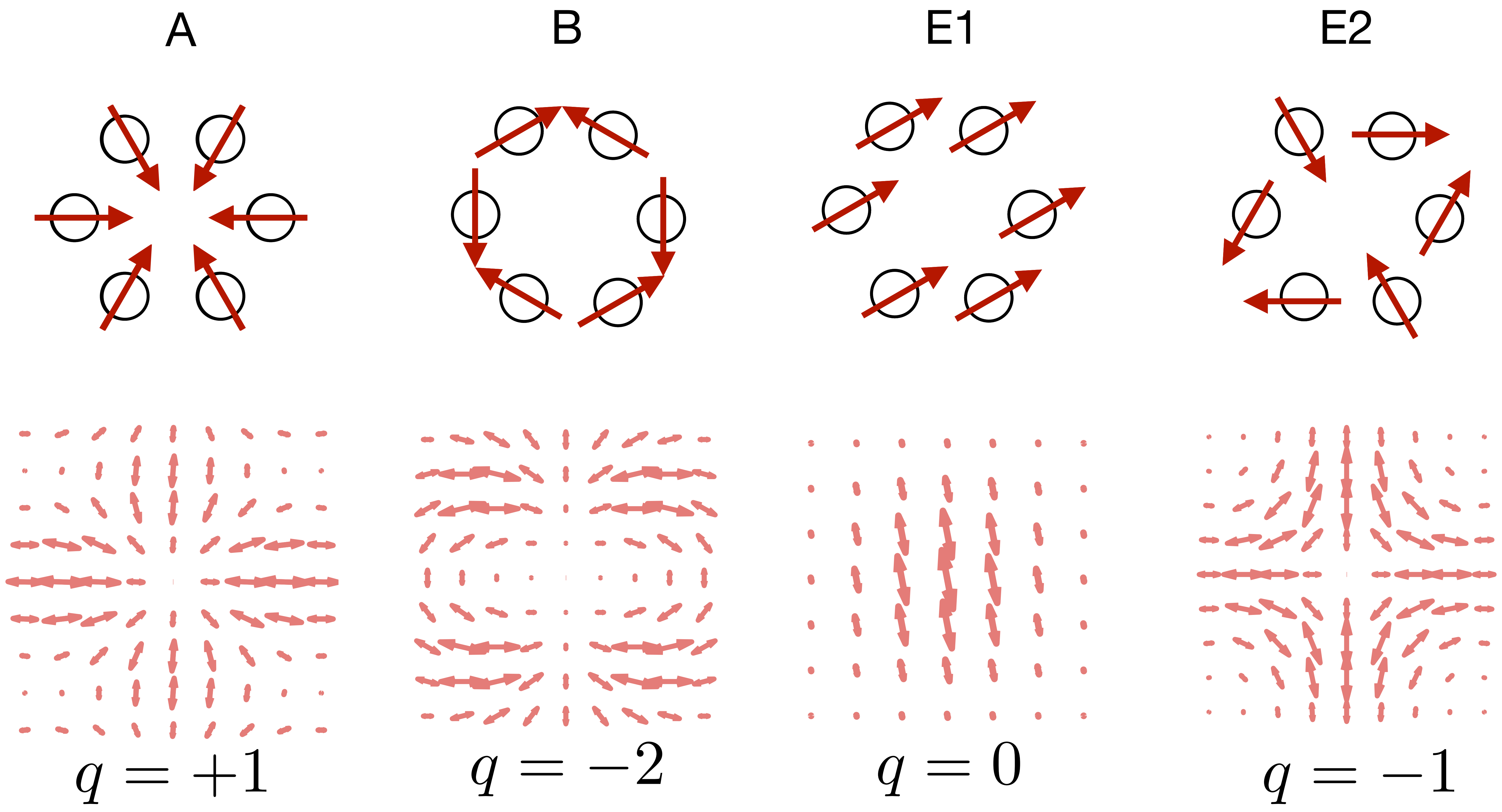

Symmetry protection of BICs

Group theory and irreducible representation

$$q_{irrep} = 1 - \frac{n}{2\pi} \arg\left(\epsilon_{irrep}\right)$$

Symmetry	irrep	$\arg(\epsilon_{\text{irrep}})$	q
C_2	A	0	$+1$
	B	π	0
C_3	A	0	$+1$
	E^*	$2\pi/3$	0
C_4	A	0	$+1$
	B	π	-1
	E^*	$\pi/2$	0
C_6	A	0	$+1$
	B	π	-2
	E_1^*	$\pi/3$	0
	E_2^*	$2\pi/3$	-1
C_8	A	0	$+1$
	B	π	-3
	E_1^*	$\pi/4$	0
	E_2^*	$\pi/2$	-1
	E_3^*	$3\pi/4$	-2

GS *et al., Phys. Rev. Lett.* **129** 173901 (2022)

Applications of BICs

Lasers and condensates of light with lower threshold

BICs laser: due to high-Q an even more efficient way of trapping light!

Also ideal for **Bose-Einstein condensates** with low thresholds in exciton polariton structures.

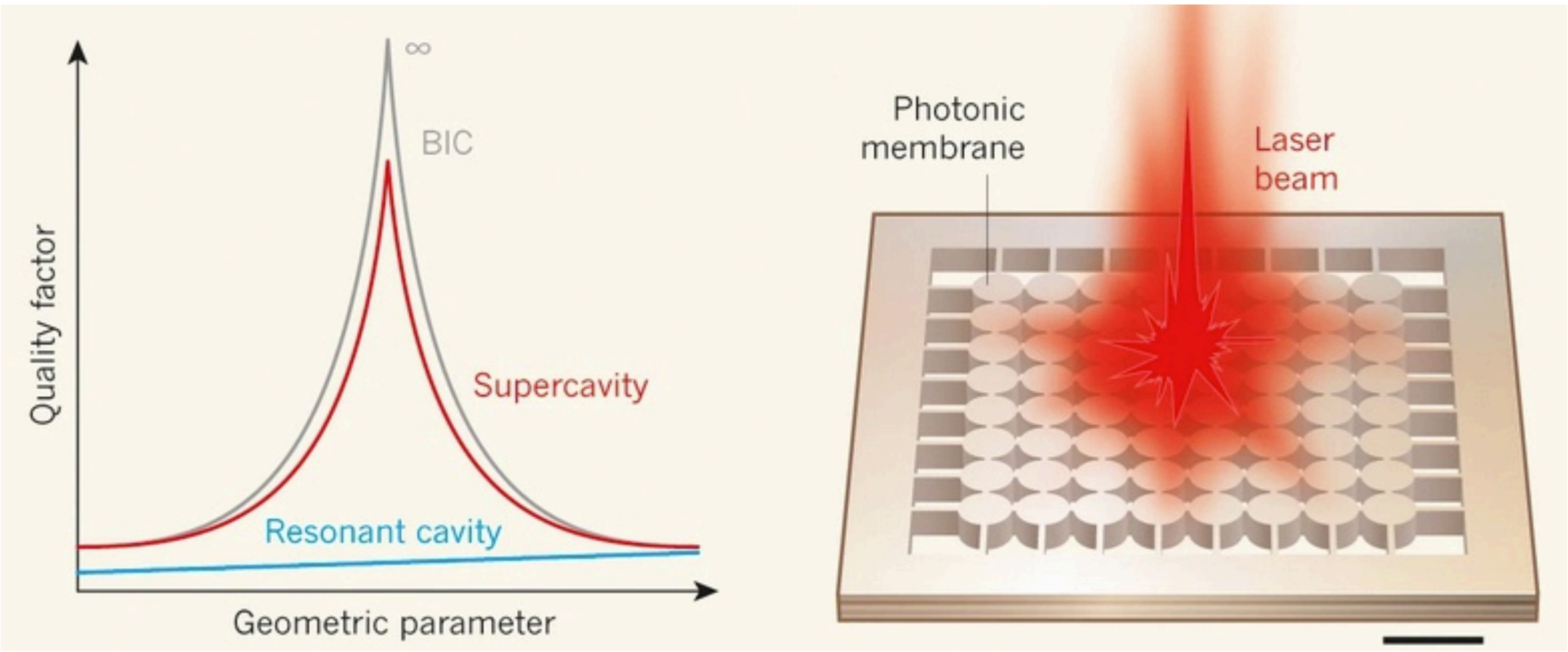

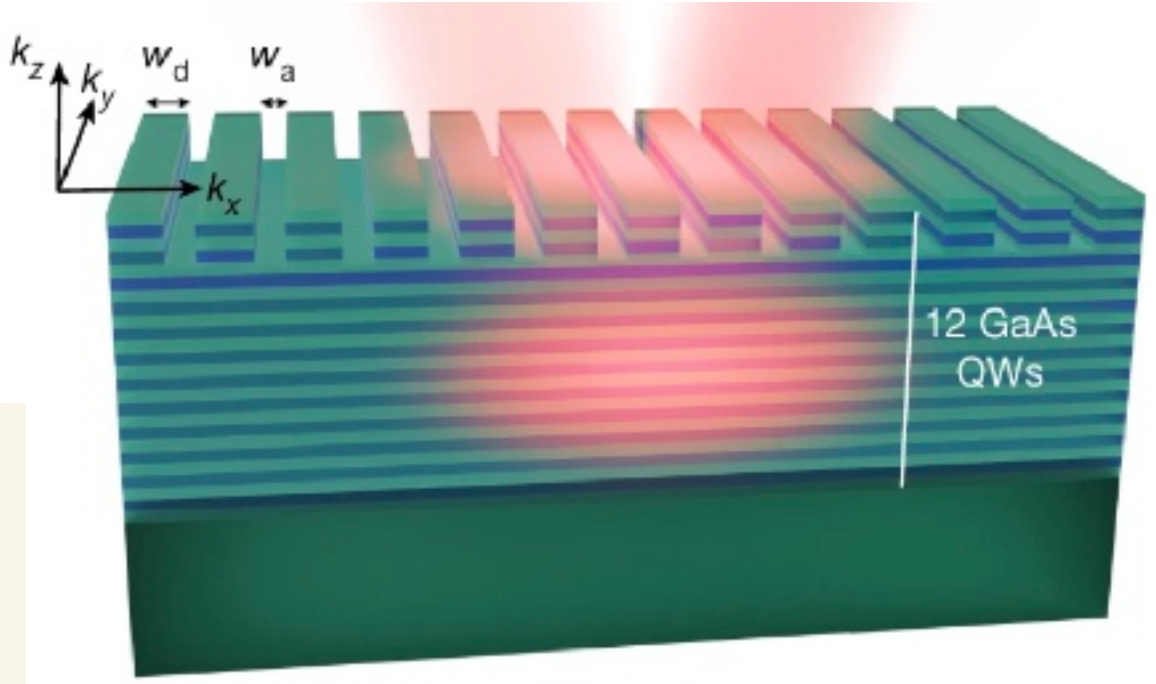

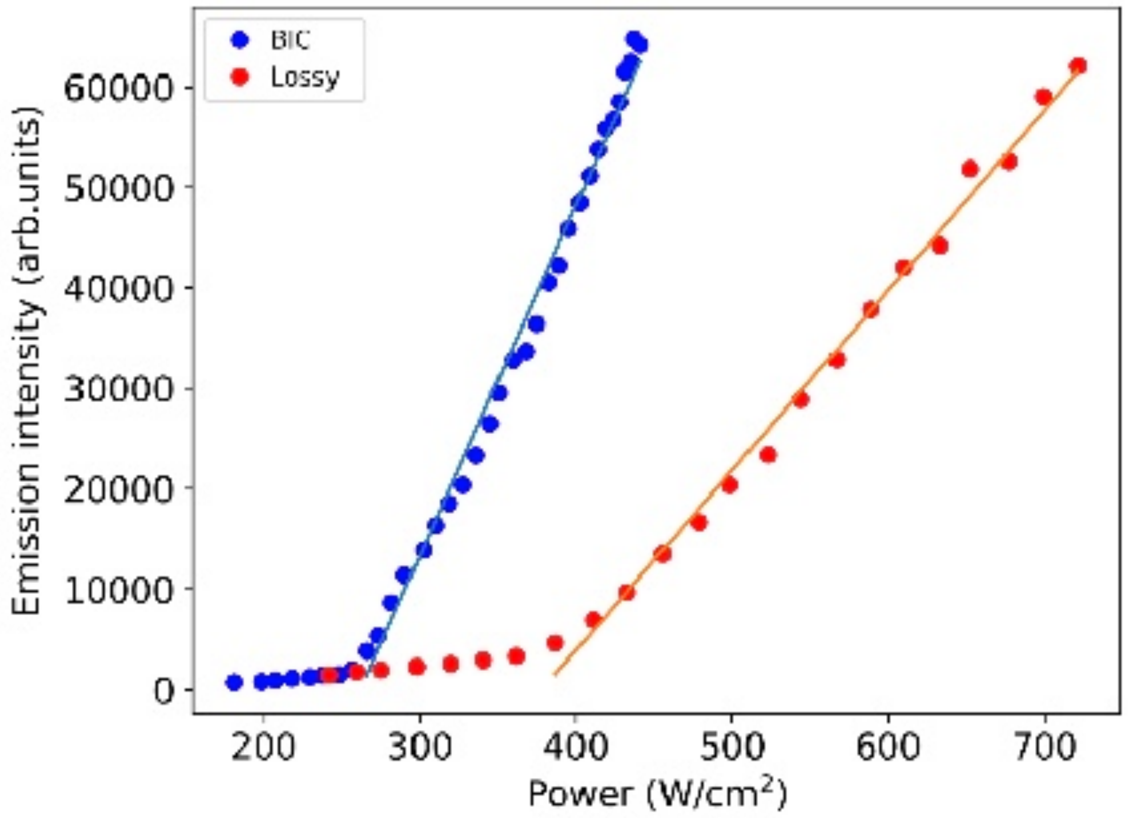

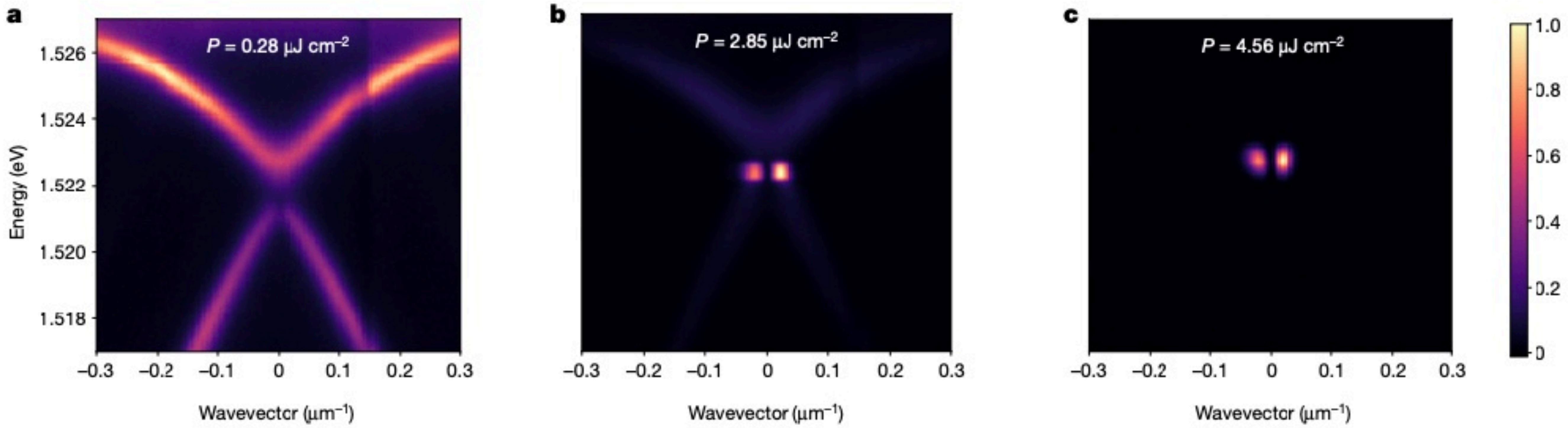

Kodigala *et al.*, *Nature* **541**, 196 (2017)
Ha *et al., Nat. Nanotechnol.* **13**, 1042 (2018)
Huang *et al.*, *Science* **367**, 1018 (2020)

Ardizzone *et al.*, *Nature* **605**, 447 (2022)
Riminucci *et al., Phys. Rev. Lett.* **131**, 246901 (2023)

Applications of BICs

A source of optical vortex beams

Bound states in the continuum can carry protected **optical angular momentum**, making them of interest for applications in spin-texture imprinting or multiplexing.

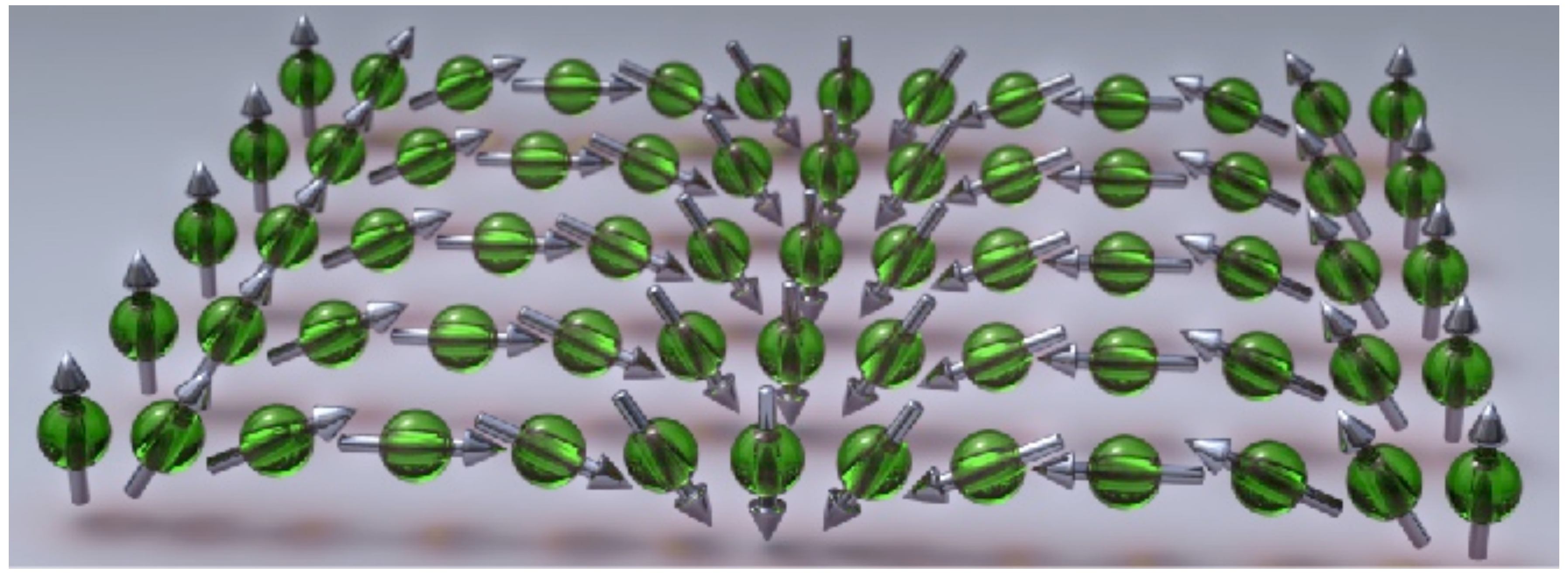

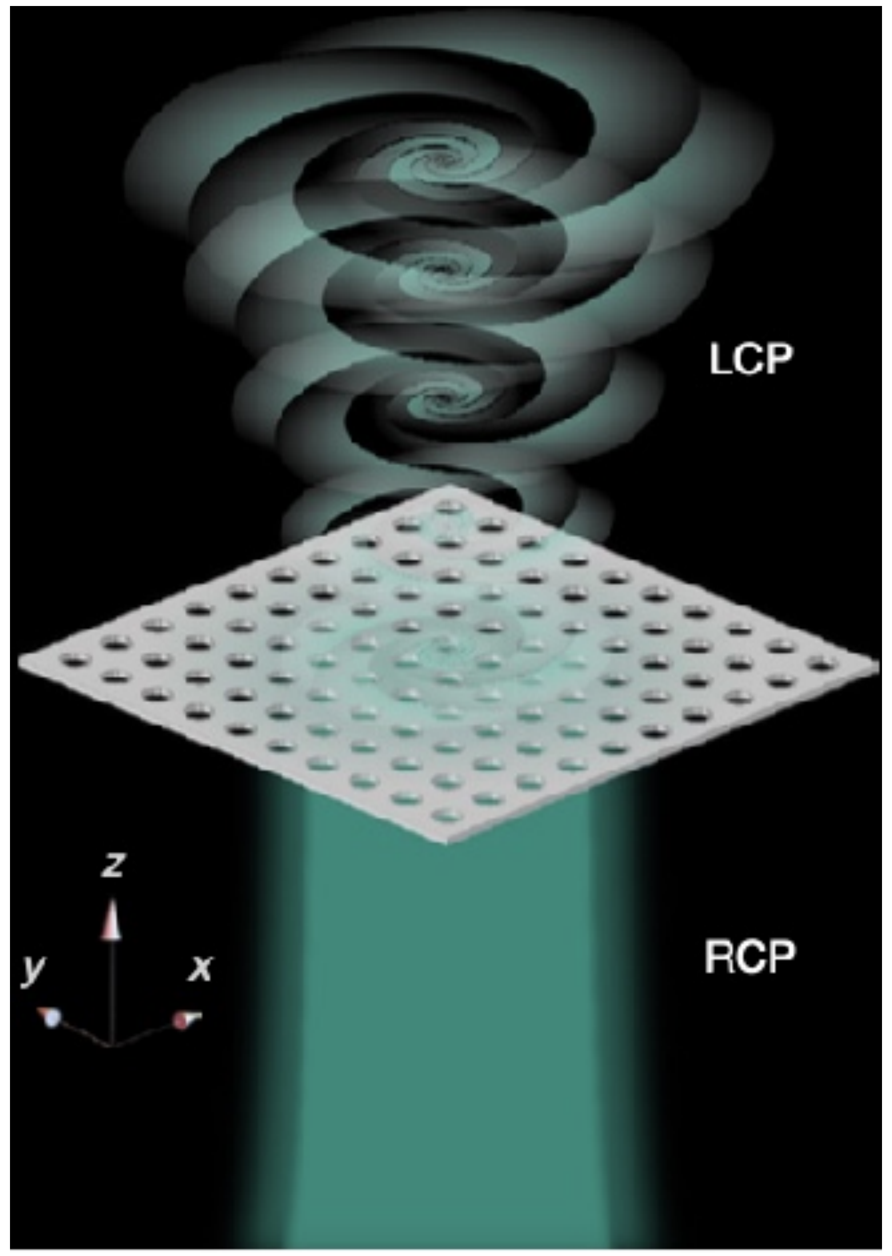

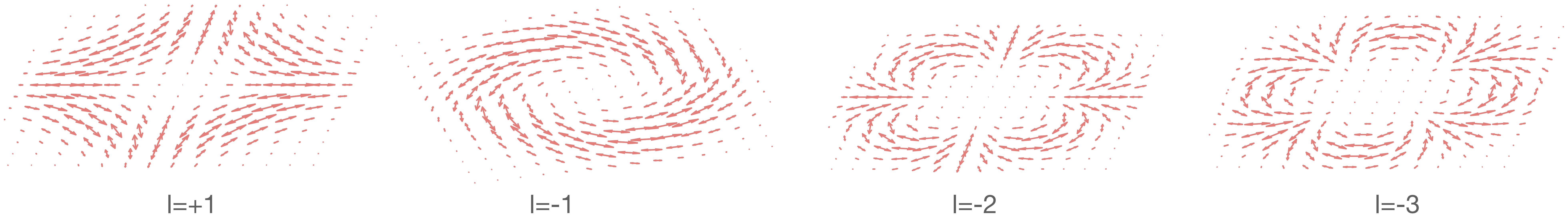

Wang *et al., Nat. Phot.* **14**, 623 (2020)
Wu *et al., New J. Phys.* **24**, 033002 (2022)
Kang *et al., Adv. Optical Mater.* **10**, 2101497 (2022)
Ishihara *et al.*, *Phys. Rev. Lett.* **130**, 126701 (2023)

Non-Hermitian topology in the far field

X. Yuan, L. Malgrey, H. Sigurðsson, H.S. Nguyen, and G. Salerno, *Physical Review Research* ***7**, 043141* (2025)
G. Salerno, Perspective on *Applied Physics Letters*, **127**, 080501 (2025)

Guided resonance modes expansion

Building an effective Hamiltonian

Consider small perturbations on top of a uniform material

$\epsilon(\mathbf{r}) \approx \epsilon + \delta\epsilon(\mathbf{r})$

We can simplify the generalized eigenvalue problem

to a standard eigenvalue equation $\hat{H}_{\text{eff}}(\mathbf{k})|\psi(\mathbf{k})\rangle = \omega|\psi(\mathbf{k})\rangle$

$$[H_{\text{eff}}(\mathbf{k})]_{\mathbf{G},\mathbf{G}'} \approx |\mathbf{k}+\mathbf{G}|\delta_{\mathbf{G},\mathbf{G}'} + \delta\epsilon_{\mathbf{G}-\mathbf{G}'}$$

Light cones "emanating" from the guided modes (Empty lattice approximation)

Coupling of guided modes

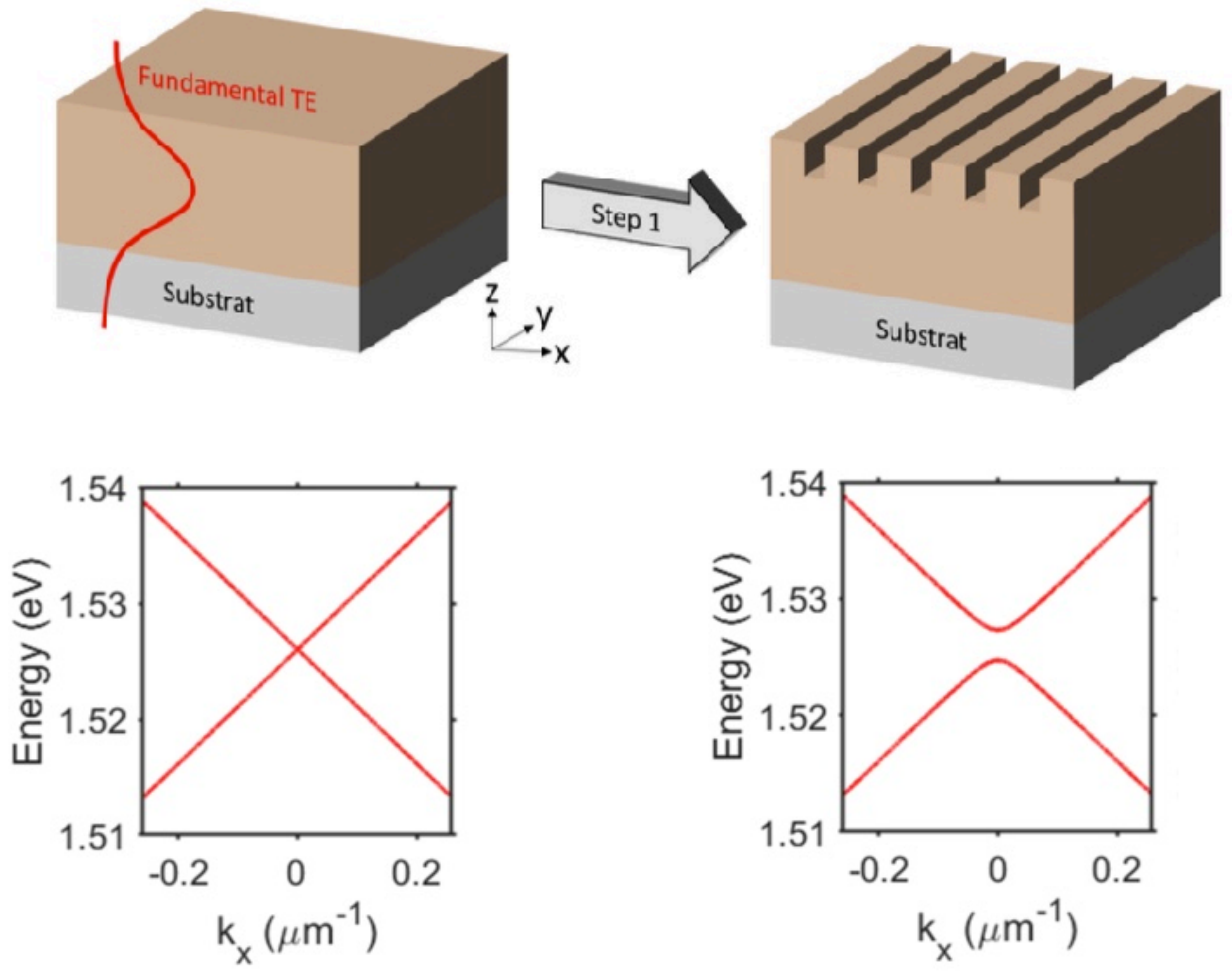

Ardizzone et al., *Nature* **605**, 447 (2022)

Two coupled levels coupled to a continuum

Origin of radiative coupling

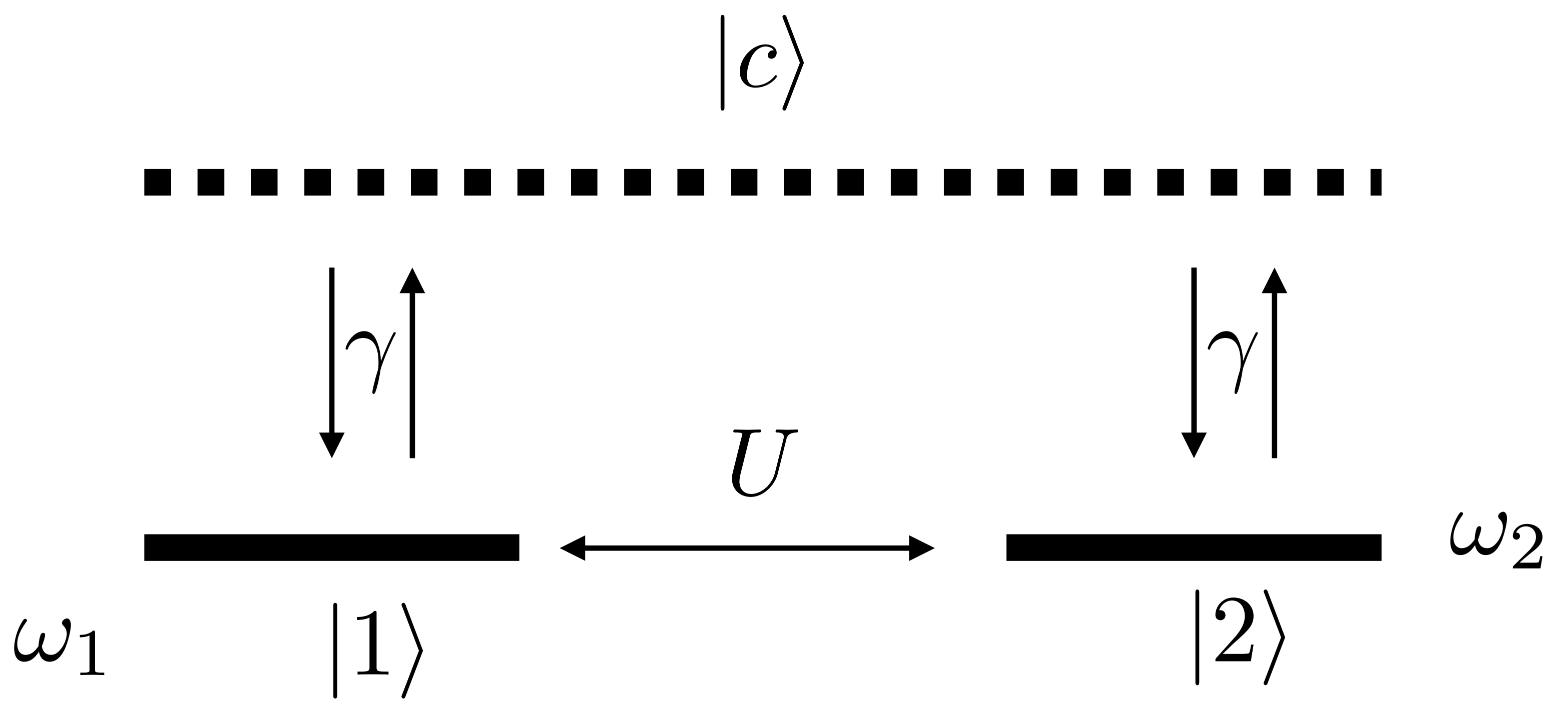

Hermitian Hamiltonian

$$H = \omega_j |j\rangle\langle j| + U|1\rangle\langle 2| + U|2\rangle\langle 1|$$

Jump operators

$$\hat{L}_j = \sqrt{\gamma}|c\rangle\langle j| - \sqrt{\gamma}|j\rangle\langle c|$$

Using the formalism of Lindblad Master Equation

$$\dot{\rho} = -i[H,\rho] + \sum_i \gamma \left(\hat{L}_i \rho \hat{L}_i^\dagger - \frac{1}{2}\hat{L}_i^\dagger \hat{L}_i \rho - \frac{1}{2}\rho \hat{L}_i^\dagger \hat{L}_i \right) =$$

$$-i\left(H_{\text{eff}}\rho - \rho H_{\text{eff}}^\dagger\right) + \sum_i \gamma \hat{L}_i \rho \hat{L}_i^\dagger$$

The effective non-Hermitian Hamiltonian (neglecting the quantum jumps)

$$H_{\text{eff}} = H - i\frac{\gamma}{2}\sum_i \hat{L}_i^\dagger \hat{L}_i = \begin{pmatrix} \omega_1 & U \\ U & \omega_2 \end{pmatrix} + i\gamma \begin{pmatrix} 1 & -1 \\ -1 & 1 \end{pmatrix}$$

mode loss +
non-Hermitian “radiative” coupling

If $\omega_1 = \omega_2$ | pure real $\epsilon_1 = \omega + U$ | cannot decay
 | complex $\epsilon_2 = \omega - U + 2i\gamma$ | can decay

Non-Hermitian effective Hamiltonian

BICs as lossless modes — 1D slab

Consider 2 guided modes spanned by **G** each with its polarization vector

$$\mathbf{G}_+ = (1,0) \qquad \mathbf{G}_- = (-1,0)$$
$$\mathbf{p}_+ \approx (0,1) \qquad \mathbf{p}_- \approx (0,-1)$$

$$\delta\epsilon_{\mathbf{G}_+ - \mathbf{G}_-} = u$$
$$\hat{\mathcal{H}}(k_x,k_y) = \begin{pmatrix} |\mathbf{k}+\mathbf{G}_+| & u \\ u & |\mathbf{k}+\mathbf{G}_-| \end{pmatrix}$$

The radiation (non-Hermitian) part of the model

$$\hat{\mathcal{H}}_{\mathrm{rad}} = i\gamma \begin{pmatrix} \mathbf{p}_+\cdot\mathbf{p}_+ & \mathbf{p}_+\cdot\mathbf{p}_- \\ \mathbf{p}_-\cdot\mathbf{p}_+ & \mathbf{p}_-\cdot\mathbf{p}_- \end{pmatrix} = i\gamma \begin{pmatrix} 1 & -1 \\ -1 & 1 \end{pmatrix}$$

$$\hat{\mathcal{H}}_{\mathrm{tot}}(k_x,k_y) \approx \begin{pmatrix} k_x & u \\ u & -k_x \end{pmatrix} + i\gamma \begin{pmatrix} 1 & -1 \\ -1 & 1 \end{pmatrix}$$

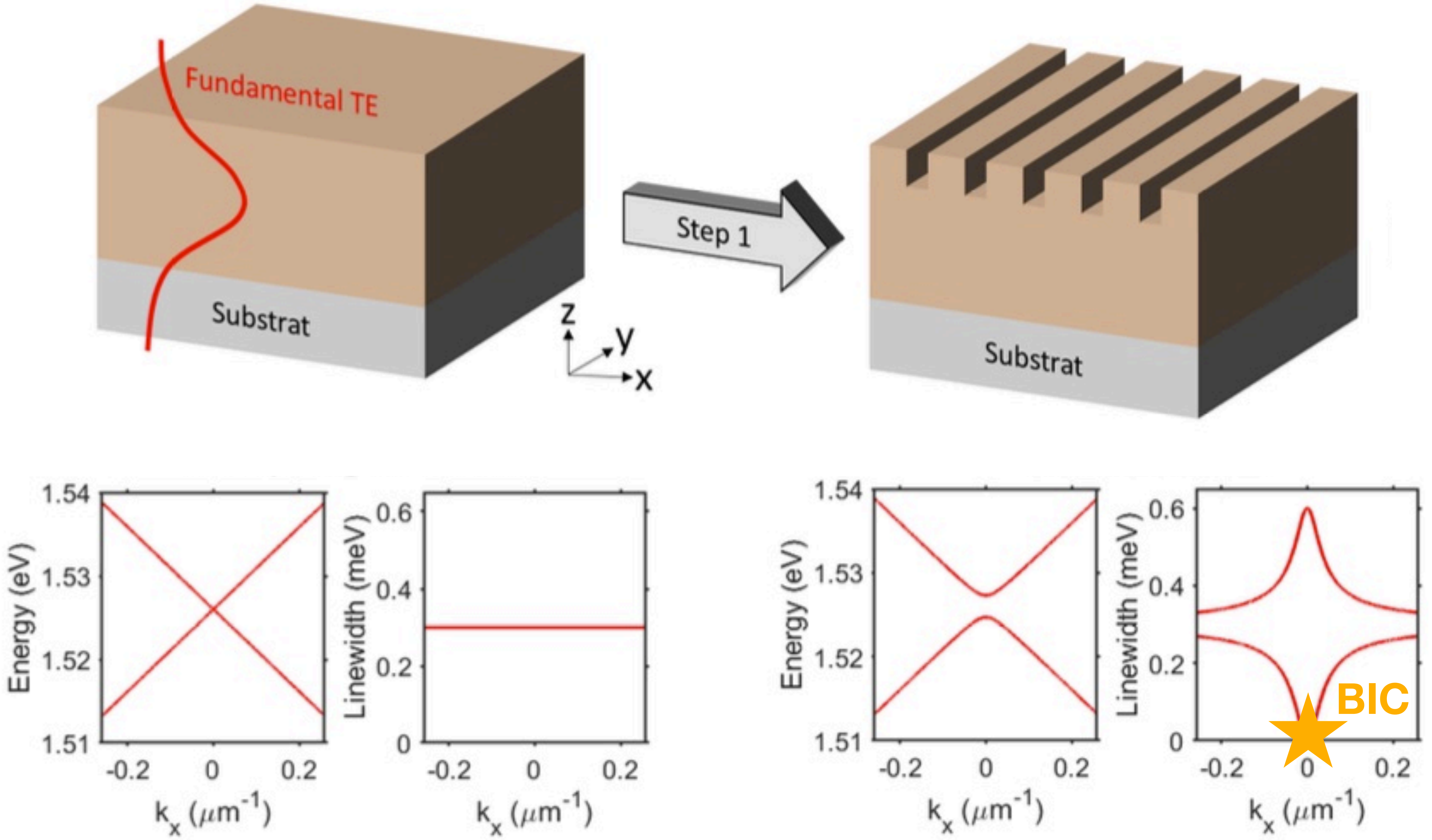

Sigurðsson, H.C. Nguyen & H.S. Nguyen, *Nanophotonics* **13**, 3503 (2023)

Ardizzone et al., *Nature* **605**, 447 (2022)

Non-Hermitian effective Hamiltonian

BICs as lossless modes — 2D slab

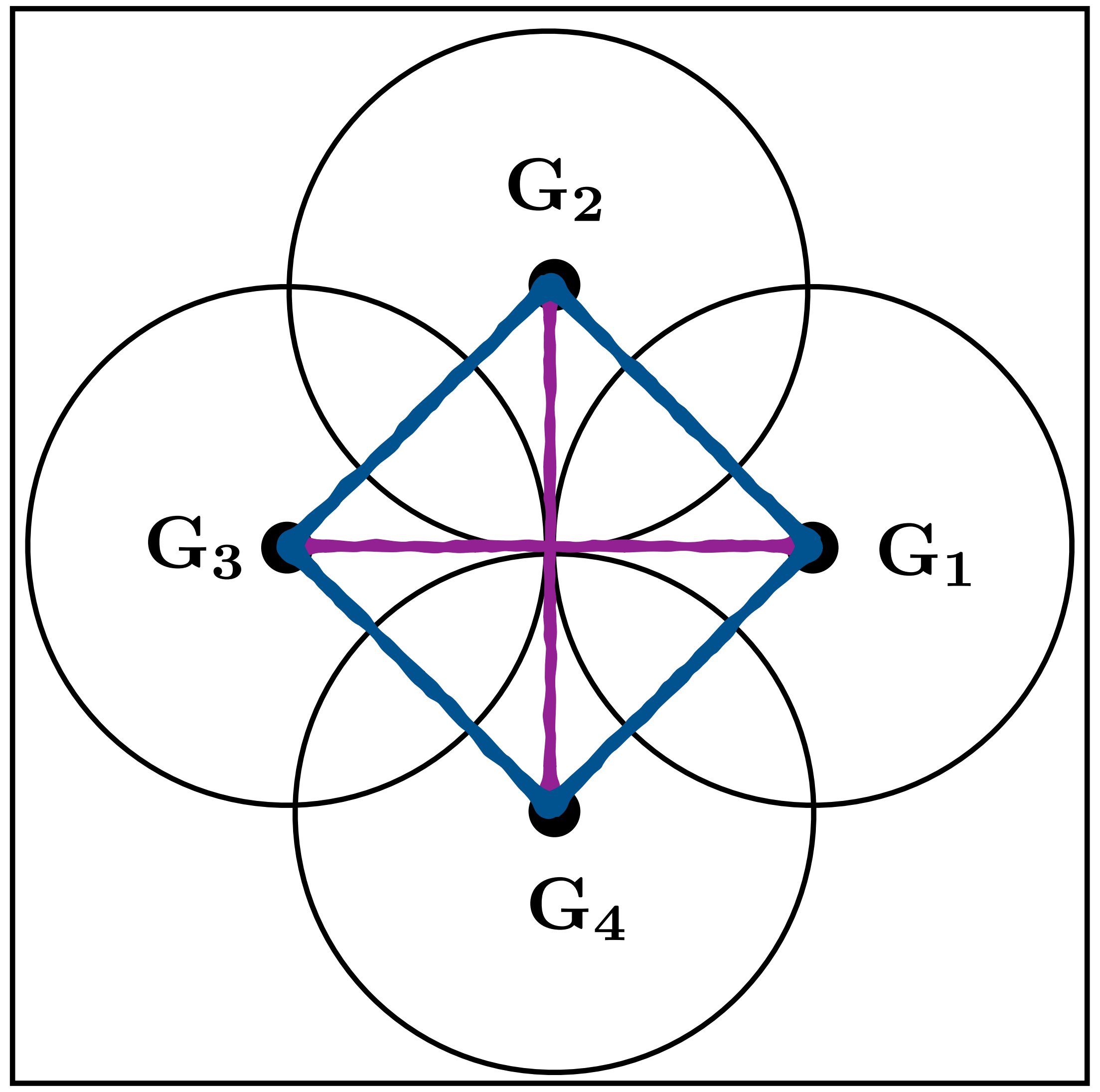

$$\begin{aligned}\mathbf{G}_1 &= (1,0)\,, & \mathbf{p}_1 &\approx (0,1)\\ \mathbf{G}_2 &= (0,1)\,, & \mathbf{p}_2 &\approx (-1,0)\\ \mathbf{G}_3 &= (-1,0)\,, & \mathbf{p}_3 &\approx (0,-1)\\ \mathbf{G}_4 &= (0,-1)\,, & \mathbf{p}_4 &\approx (-1,0)\end{aligned}$$

$$\begin{aligned}\varepsilon_{\mathbf{G_1}-\mathbf{G_2}} = \varepsilon_{\mathbf{G_2}-\mathbf{G_3}} &= v\\ \varepsilon_{\mathbf{G_3}-\mathbf{G_4}} = \varepsilon_{\mathbf{G_4}-\mathbf{G_1}} &= v\\ \varepsilon_{\mathbf{G_1}-\mathbf{G_3}} &= u_x\\ \varepsilon_{\mathbf{G_2}-\mathbf{G_4}} &= u_y\end{aligned}$$

$$\hat{\mathcal{H}}(k_x,k_y) = \begin{pmatrix} |\mathbf{k}+\mathbf{G}_1| & v & u_x & v\\ v & |\mathbf{k}+\mathbf{G}_2| & v & u_y\\ u_x & v & |\mathbf{k}+\mathbf{G}_3| & v\\ v & u_y & v & |\mathbf{k}+\mathbf{G}_4| \end{pmatrix}$$

Yuan, GS et al., *Phys. Rev. Research* ***7****, 043141* (2025)

V. A. Nguyen et al., *arXiv:2507.20033* (2025)

Non-Hermitian effective Hamiltonian

BICs as lossless modes — 2D slab

$$\hat{\mathcal{H}}(k_x,k_y)=\begin{pmatrix}|\mathbf{k}+\mathbf{G}_1| & v & u_x & v\\ v & |\mathbf{k}+\mathbf{G}_2| & v & u_y\\ u_x & v & |\mathbf{k}+\mathbf{G}_3| & v\\ v & u_y & v & |\mathbf{k}+\mathbf{G}_4|\end{pmatrix}$$

$$\mathbf{G}_1=(1,0)\,,\qquad \mathbf{p}_1\approx(0,1)\qquad\qquad \mathbf{G}_3=(-1,0)\,,\qquad \mathbf{p}_3\approx(0,-1)$$
$$\mathbf{G}_2=(0,1)\,,\qquad \mathbf{p}_2\approx(-1,0)\qquad\qquad \mathbf{G}_4=(0,-1)\,,\qquad \mathbf{p}_4\approx(-1,0)$$

$$\hat{\mathcal{H}}_{\mathrm{rad}}=i\gamma\begin{pmatrix}\mathbf{p}_1\cdot\mathbf{p}_1 & \mathbf{p}_1\cdot\mathbf{p}_2 & \mathbf{p}_1\cdot\mathbf{p}_3 & \mathbf{p}_1\cdot\mathbf{p}_4\\ \mathbf{p}_2\cdot\mathbf{p}_1 & \mathbf{p}_2\cdot\mathbf{p}_2 & \mathbf{p}_2\cdot\mathbf{p}_3 & \mathbf{p}_2\cdot\mathbf{p}_4\\ \mathbf{p}_3\cdot\mathbf{p}_1 & \mathbf{p}_3\cdot\mathbf{p}_2 & \mathbf{p}_3\cdot\mathbf{p}_3 & \mathbf{p}_3\cdot\mathbf{p}_4\\ \mathbf{p}_4\cdot\mathbf{p}_1 & \mathbf{p}_4\cdot\mathbf{p}_2 & \mathbf{p}_4\cdot\mathbf{p}_3 & \mathbf{p}_4\cdot\mathbf{p}_4\end{pmatrix}=i\gamma\begin{pmatrix}1 & 0 & -1 & 0\\ 0 & 1 & 0 & -1\\ -1 & 0 & 1 & 0\\ 0 & -1 & 0 & 1\end{pmatrix}$$

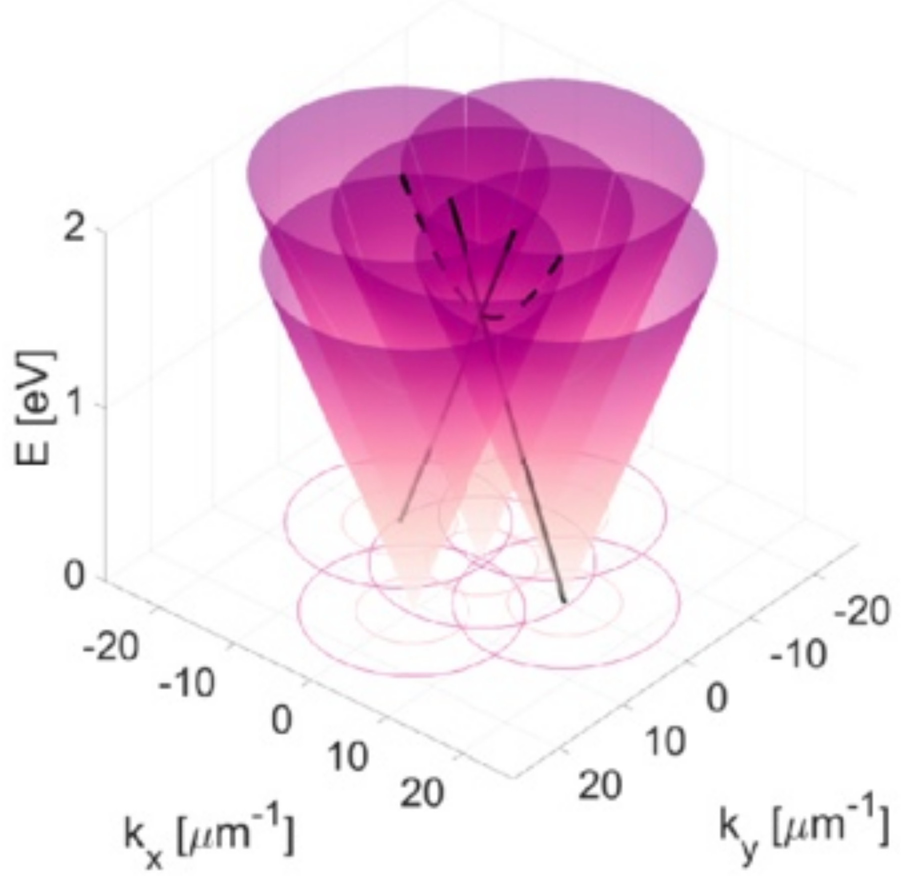

The radiation coupling is only for co-polarized field component.

Yuan, GS et al., *Phys. Rev. Research* **7**, *043141* (2025)

V. A. Nguyen et al., *arXiv:2507.20033* (2025)

Non-Hermitian effective Hamiltonian

The BICs wavefunctions

$$\hat{H}_{\text{tot}} = \begin{pmatrix} k_x + i\gamma & v & u_x - i\gamma & v \\ v & k_y + i\gamma & v & u_y - i\gamma \\ u_x - i\gamma & v & -k_x + i\gamma & v \\ v & u_y - i\gamma & v & -k_y + i\gamma \end{pmatrix}$$

$$\hat{H}_{\text{tot}}|\psi\rangle = \epsilon|\psi\rangle \qquad u_x - u_y = \delta$$

$$\epsilon^{\pm}_{\text{BIC}} = u \pm \sqrt{\delta^2 + 4v^2} \qquad \psi^{\pm}_{\text{BIC}} = \begin{pmatrix} \delta \pm \sqrt{\delta^2 + 4v^2} \\ 2v \\ \delta \pm \sqrt{\delta^2 + 4v^2} \\ 2v \end{pmatrix}$$

$$\epsilon^{\pm} = -u \pm \delta + 2i\gamma \qquad \psi^{-} = \begin{pmatrix} -1 \\ 0 \\ 1 \\ 0 \end{pmatrix} \quad \psi^{+} = \begin{pmatrix} 0 \\ -1 \\ 0 \\ 1 \end{pmatrix}$$

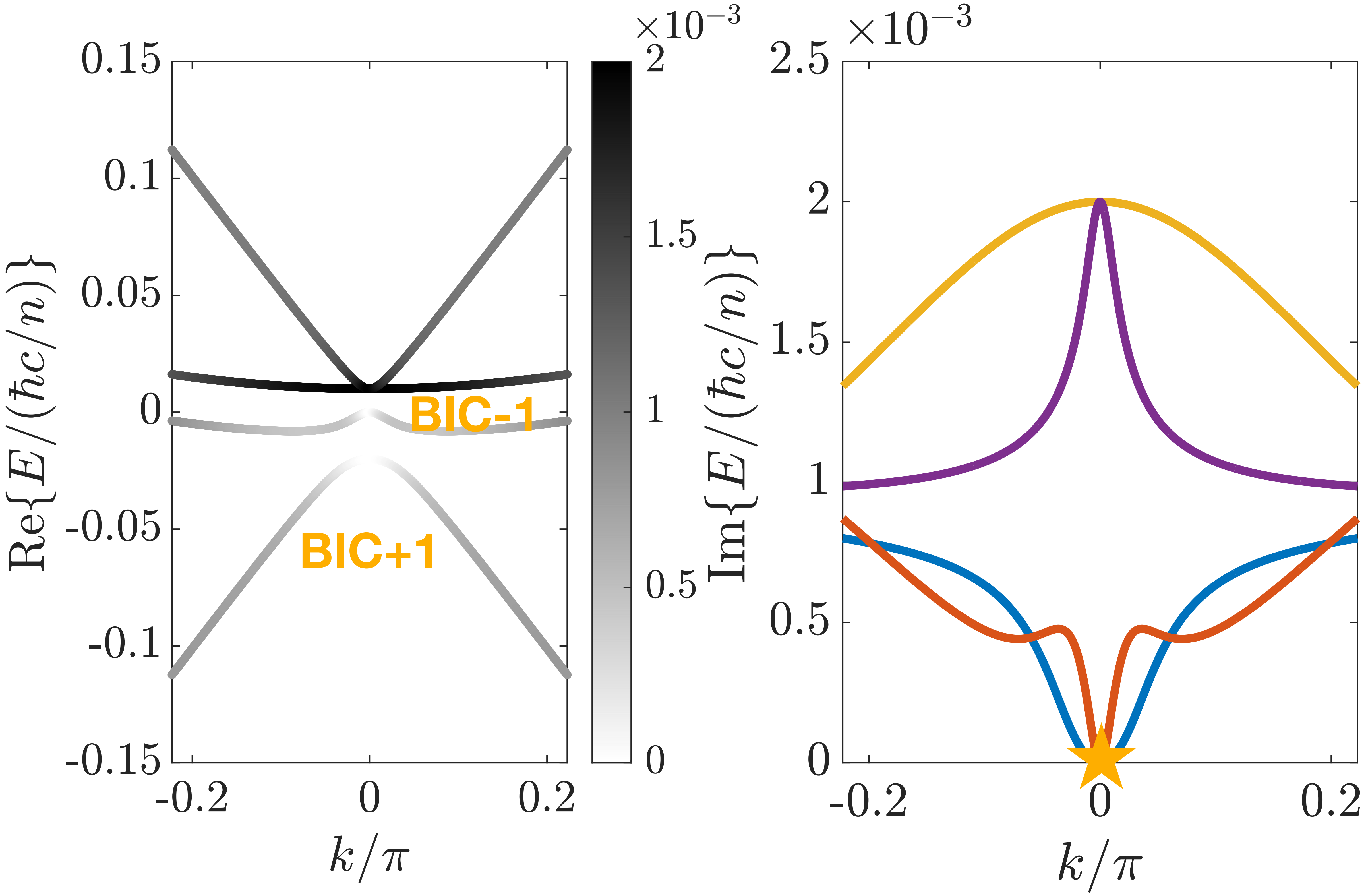

Symmetry	IR	$\arg(\epsilon_{\text{IR}})$	q
C_4	A	0	$+1$
	B	π	-1
	E^*	$\pi/2$	0

Non-Hermitian effective Hamiltonian

The electric field in the far field

Reconstruct the far-field using the polarization vectors of the guided modes $\mathbf{E} = \sum_m \psi_m \mathbf{p}_m$

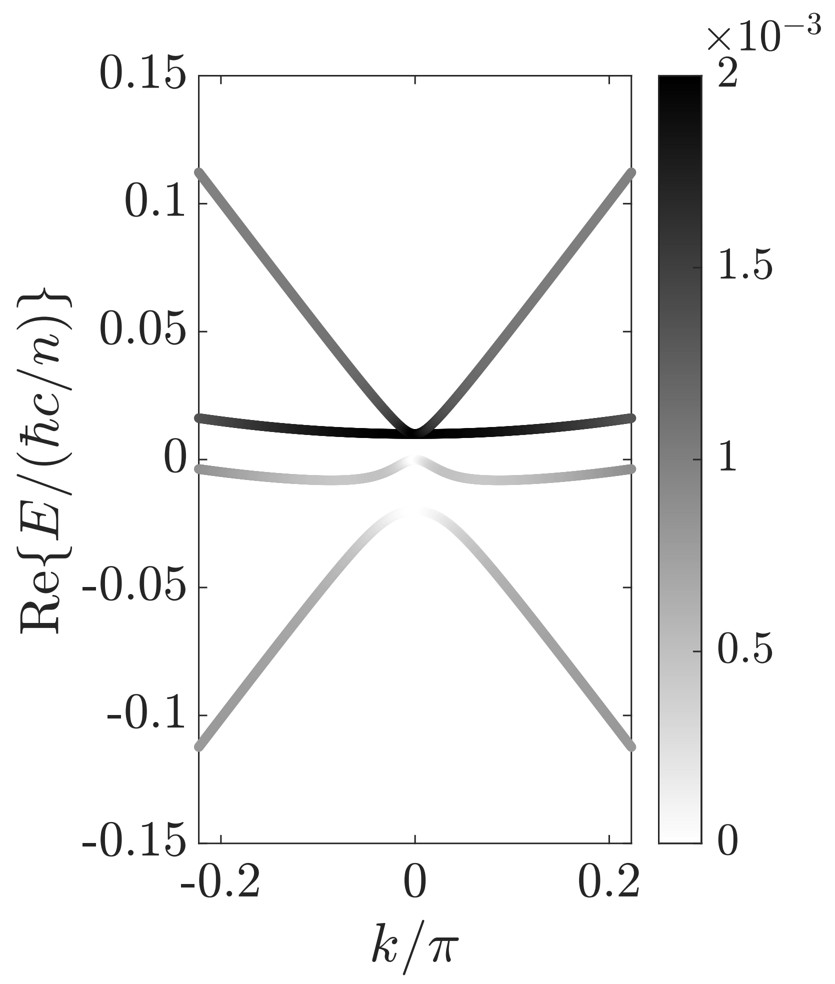

$$\psi^{\pm}_{\mathrm{BIC}} = \begin{pmatrix} \frac{\delta \pm \sqrt{\delta^2+4v^2}}{2v} \\ \frac{\delta \pm \sqrt{\delta^2+4v^2}}{2v} \end{pmatrix} \qquad \psi^{-} = \begin{pmatrix} -1 \\ 0 \\ 1 \\ 0 \end{pmatrix} \qquad \psi^{+} = \begin{pmatrix} 0 \\ -1 \\ 0 \\ 1 \end{pmatrix}$$

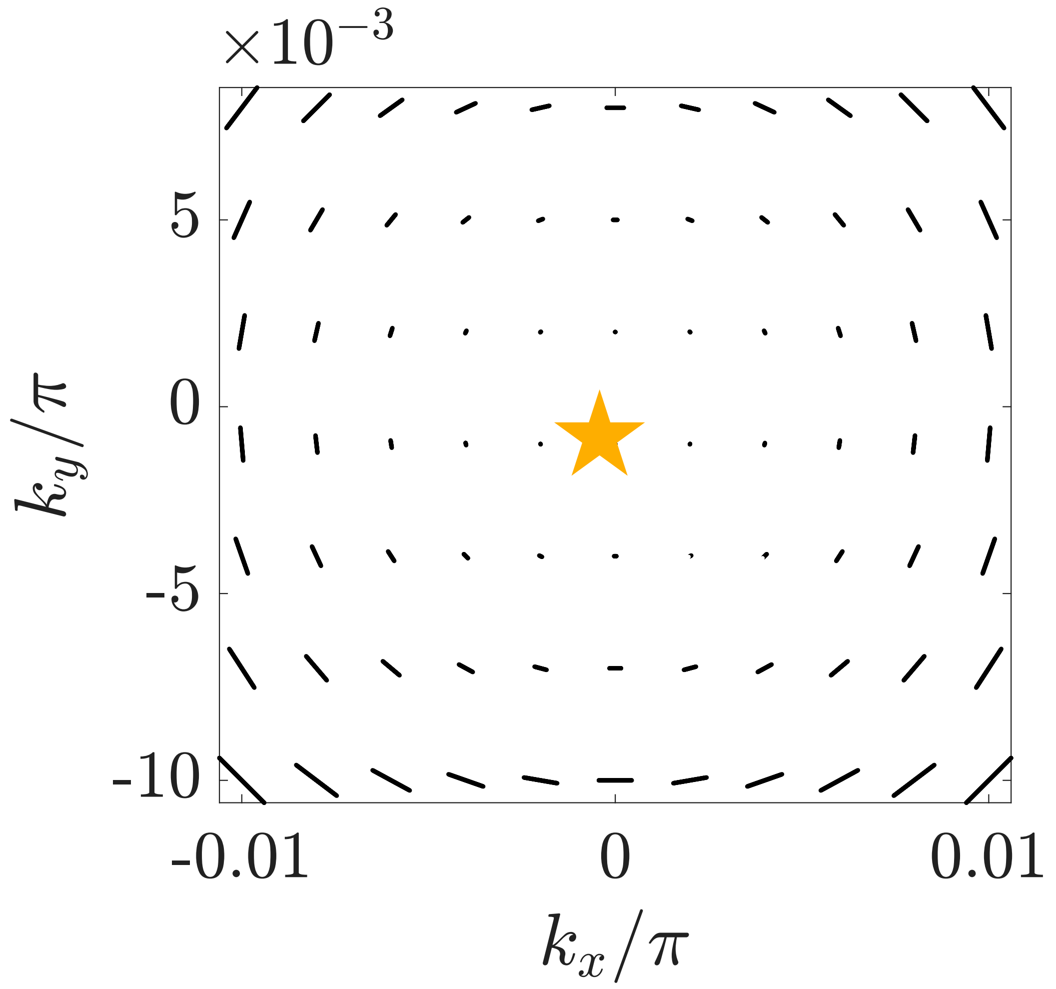

BIC q=+1

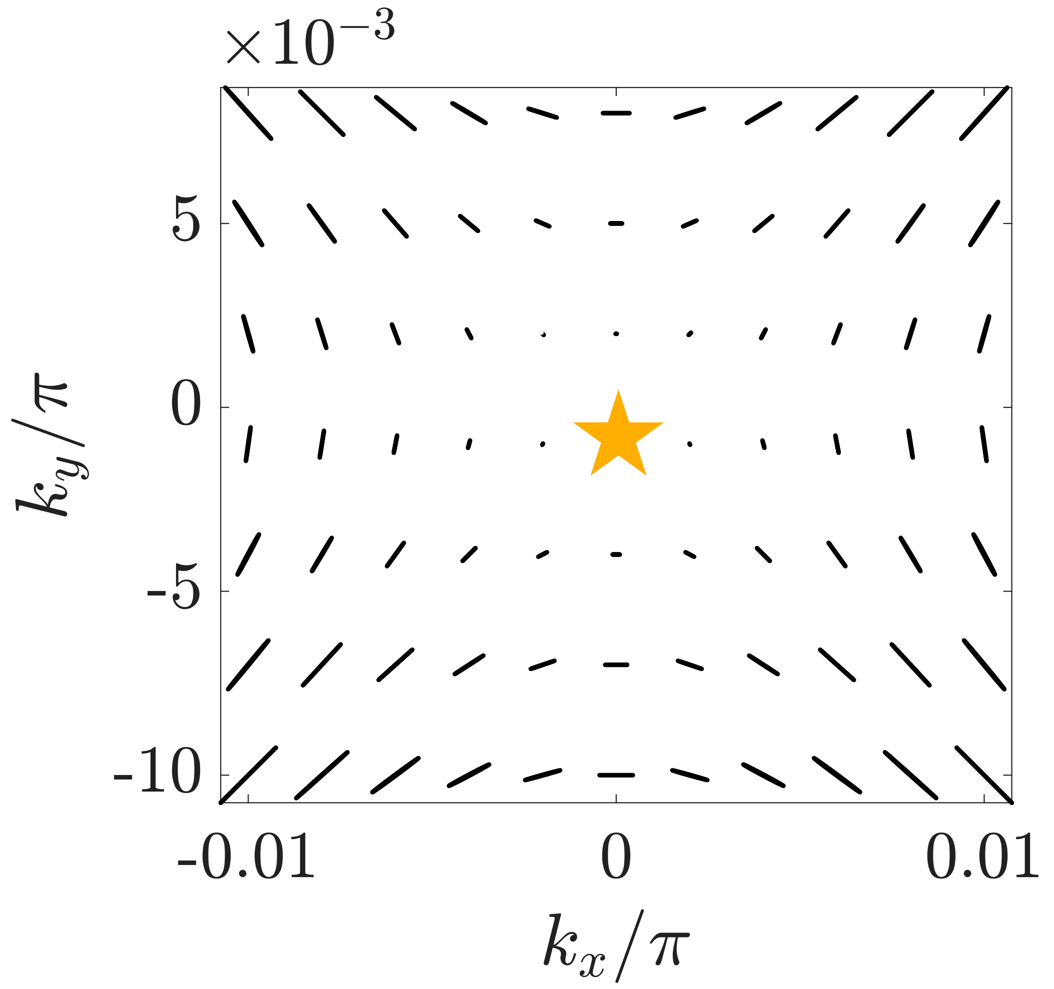

BIC q=-1

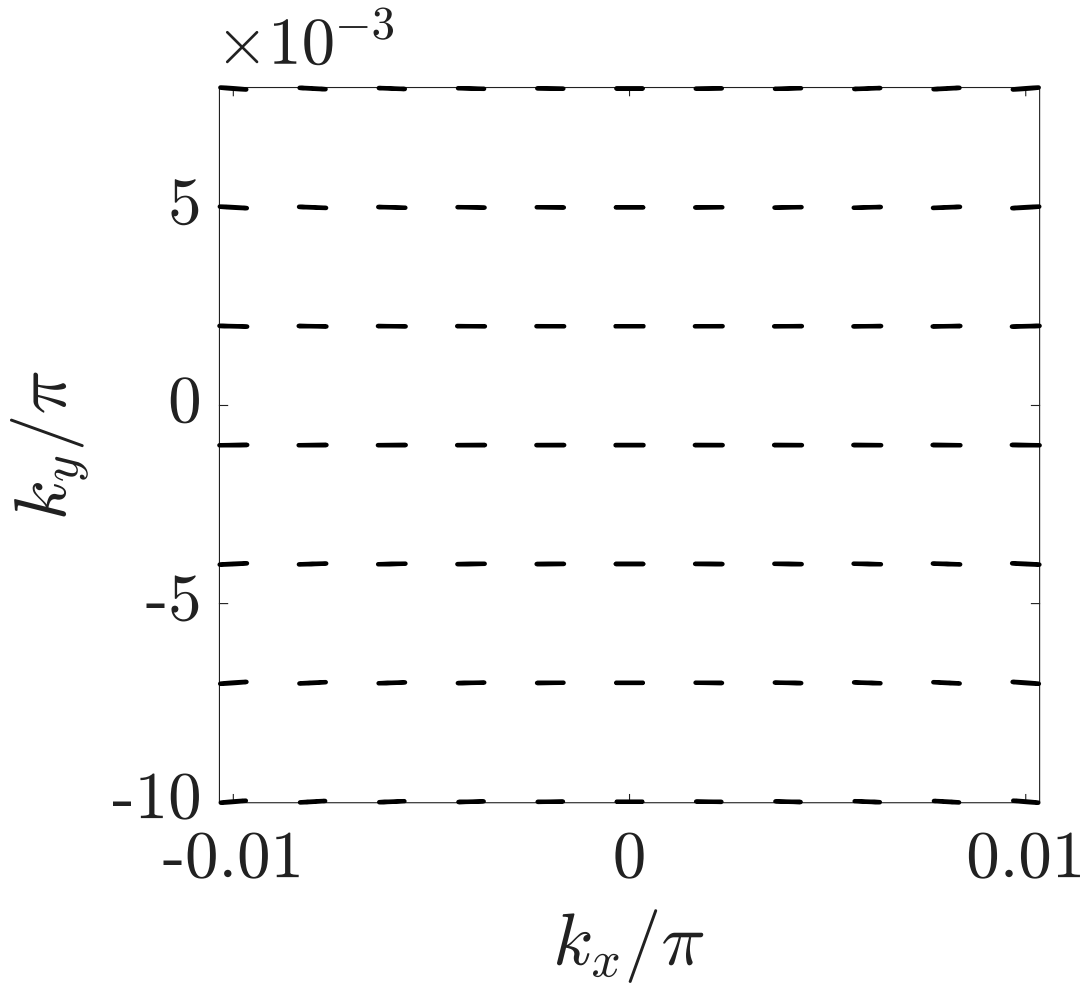

non-BIC q=0

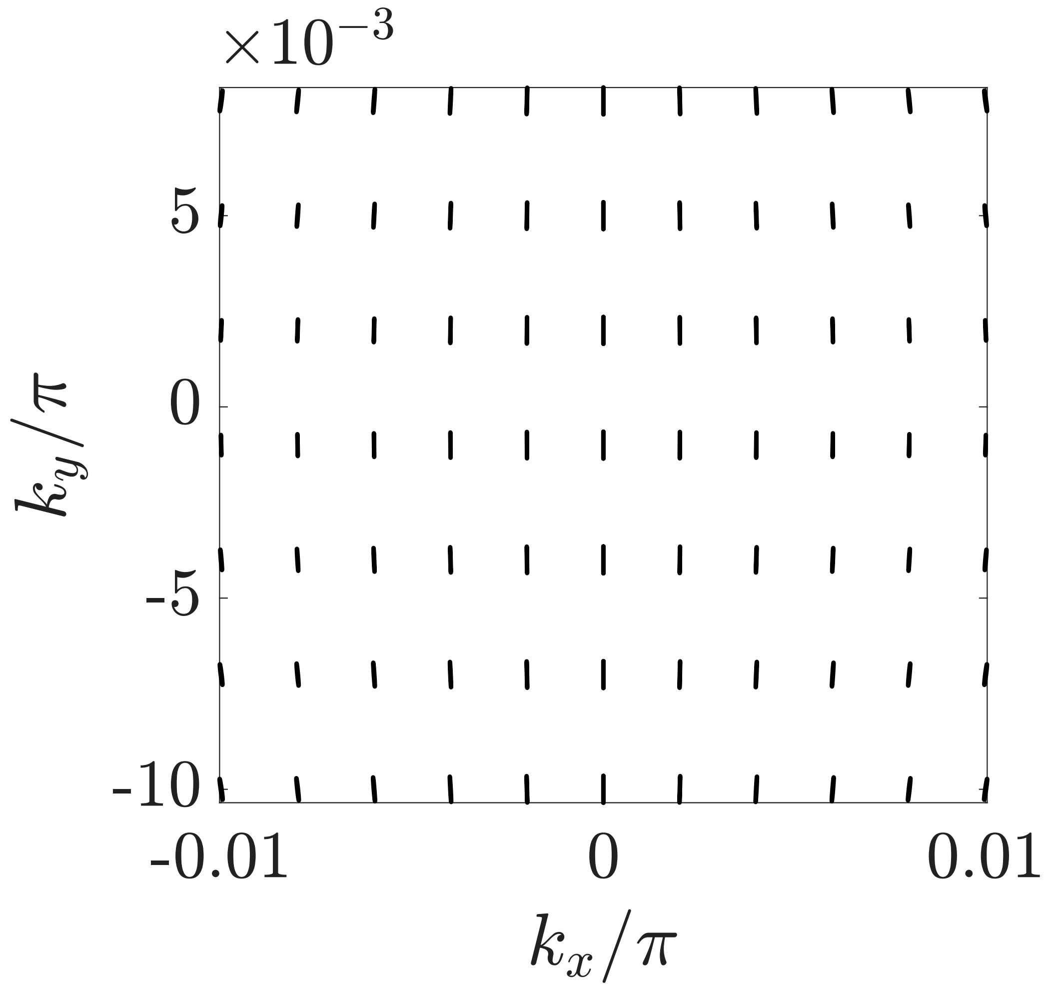

non-BIC q=0

Non-Hermitian effective Hamiltonian

Comparison with RCWA

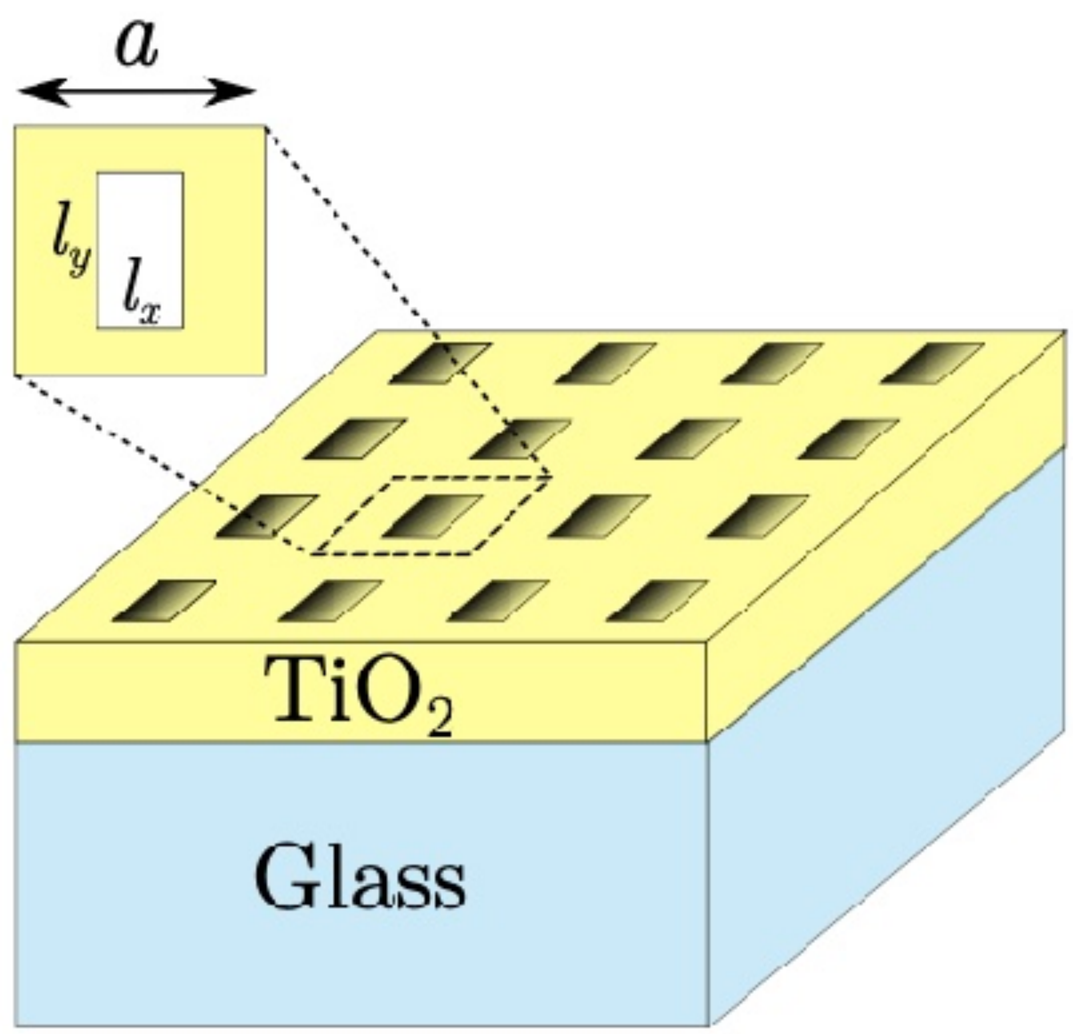

	$u_x 10^{-3}$	$u_y 10^{-3}$	$v 10^{-3}$	l_x [μm]	l_y [μm]
BBNN	-3.5	-3.5	1.1	0.12	0.12
BNBN	-13	4.5	2	0.12	0.28
BNNB	0.014	0.014	1.4	0.208	0.208
NBNB	-4.5	14	1.4	0.2	0.28
NNBB	5.6	5.6	2.4	0.28	0.28

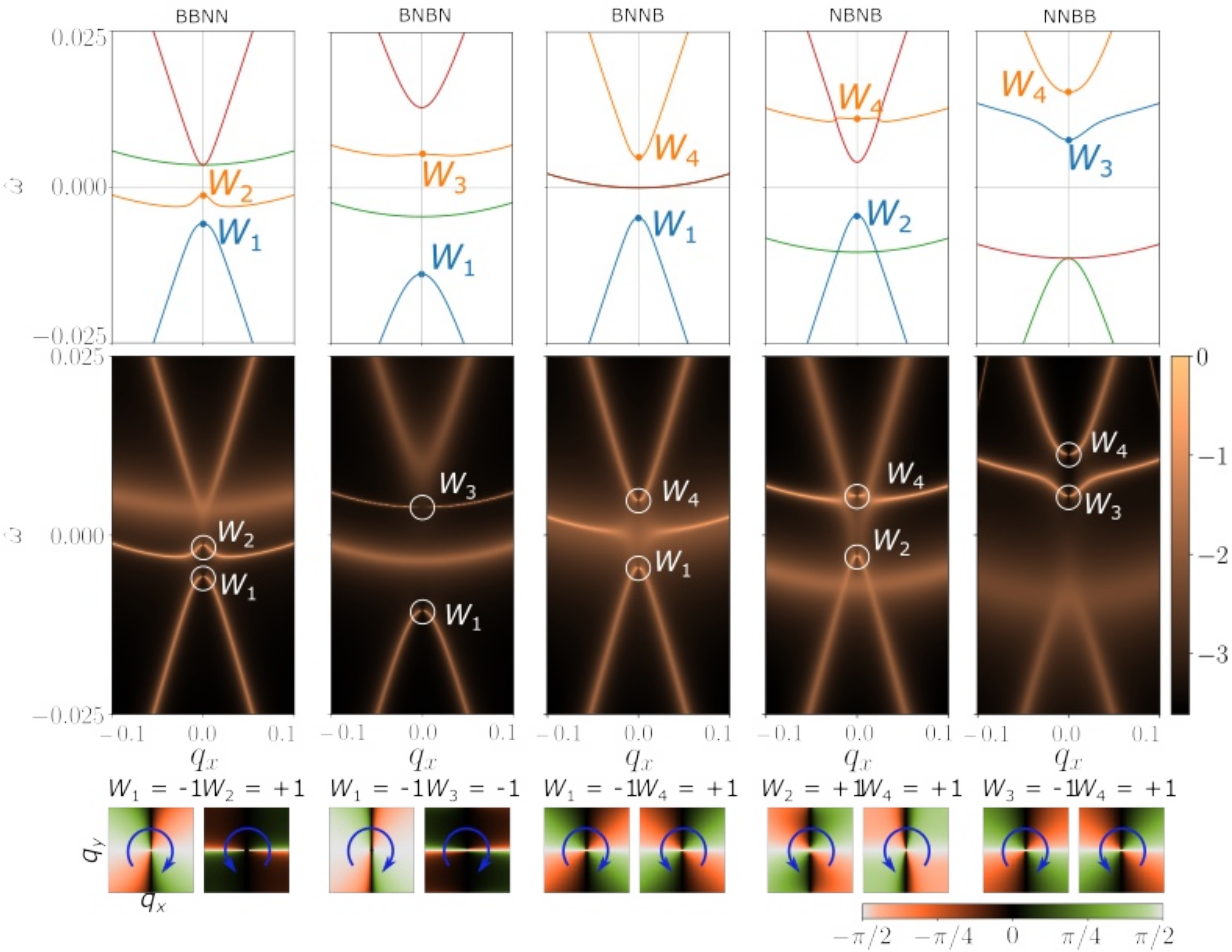

Yuan, GS et al., *Phys. Rev. Research* ***7****, 043141* (2025)

Non-Hermitian Quantum Geometric Tensor

Two ways of calculating it?

“Bulk calculated”
from the eigenstates of the effective Hamiltonian

$$\hat{H}_{\mathrm{tot}}|\psi^R\rangle = \epsilon\,|\psi^R\rangle$$
$$\hat{H}^\dagger_{\mathrm{tot}}|\psi^L\rangle = \epsilon^*|\psi^L\rangle$$

$$T^{\alpha\beta}_{\mu\nu} = \sum_{m\neq n} \frac{\langle\psi^\alpha_n|\partial_\mu \hat{H}_{\mathrm{tot}}|\psi^\beta_m\rangle\langle\psi^\alpha_m|\partial_\nu \hat{H}_{\mathrm{tot}}|\psi^\beta_n\rangle}{(\epsilon_m - \epsilon^*_n)^2}$$

Use right eigenvectors

$$B_{\mu\nu} = -\frac{1}{2}\mathrm{Im}\{T^{RR}_{\mu\nu} - T^{RR}_{\nu\mu}\}$$
$$g_{\mu\nu} = \frac{1}{2}\mathrm{Re}\{T^{RR}_{\mu\nu} + T^{RR}_{\nu\mu}\}$$

“Far-field calculated”
from Electric field polarization and the Stokes vectors

$$\mathbf{E} = \hat{P}|\psi\rangle \qquad \mathbf{S} = \langle\mathbf{E}|\sigma|\mathbf{E}\rangle$$

$$\phi = \frac{1}{2}\arctan\left(\frac{S_2}{S_1}\right) \qquad \chi = \frac{1}{2}\arctan\left(\frac{S_3}{\sqrt{S_1^2+S_2^2}}\right)$$

$$|E\rangle = \cos(\chi/2)e^{i\phi}|+\rangle + \sin(\chi/2)|-\rangle$$

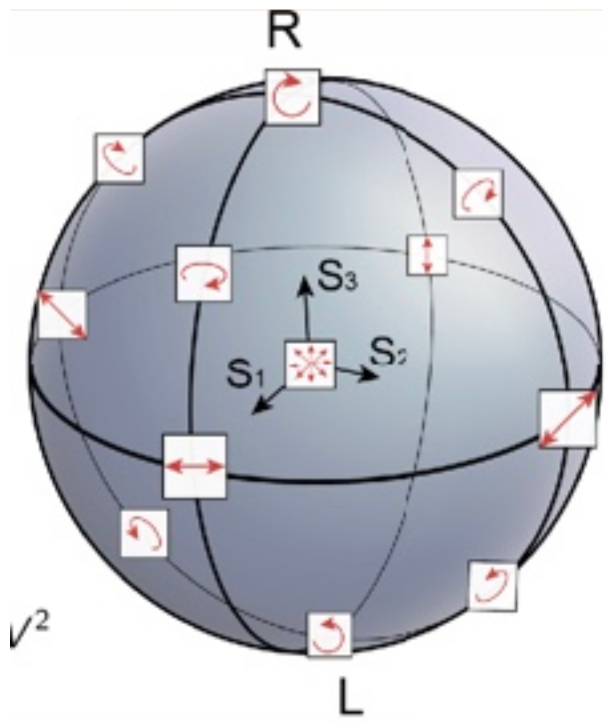

$$B_{\mu\nu} = \frac{1}{2}\sin\chi\left(\partial_\mu\chi\partial_\nu\phi - \partial_\mu\phi\partial_\nu\chi\right)$$
$$g_{\mu\nu} = \frac{1}{4}\left(\partial_\mu\chi\partial_\nu\chi + \sin^2\chi\partial_\mu\phi\partial_\nu\phi\right)$$

Bleu, Solnyshkov & Malpuech, *Phys. Rev. B* **97**, 195422 (2018)

Quantum Geometric Tensor observations

Not an abstract quantity

Microcavity exciton-polariton

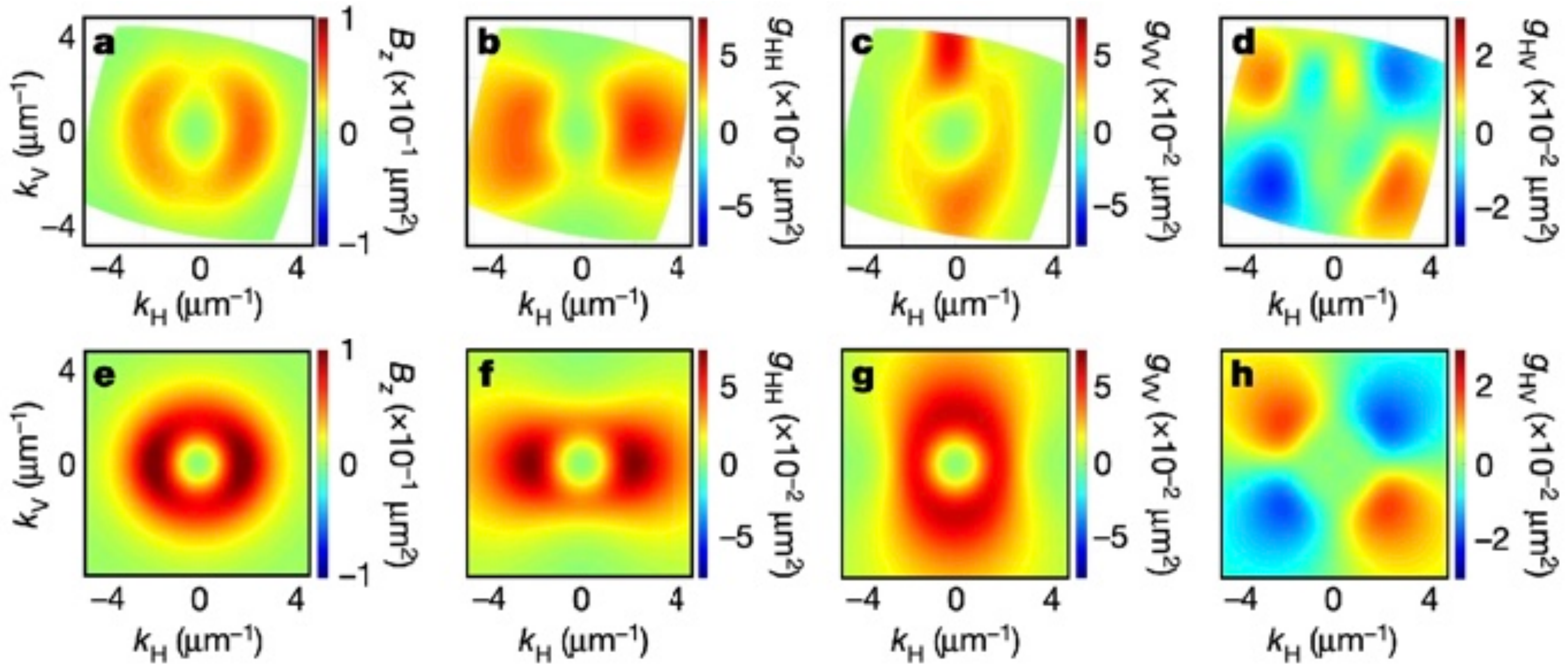

Gianfrate et al., *Nature* **578**, 381 (2020)

Other realizations (possibly an incomplete list)

Tan et al., *Phys. Rev. Lett.* **123**, 159902 (2019)

Asteria et al., *Nat. Phys.* **15**, 449 (2019)

Min et al. *Natl. Sci. Rev.* **7**, 254 (2020)

Kang et al. *Nat. Phys.* **21**, 110 (2025)

Kim et al. *Science* ***388**, 1050 (2025)*

Guillot et al., *arXiv:2507.16446* (2025)

….

Plasmonic lattices @ Aalto!

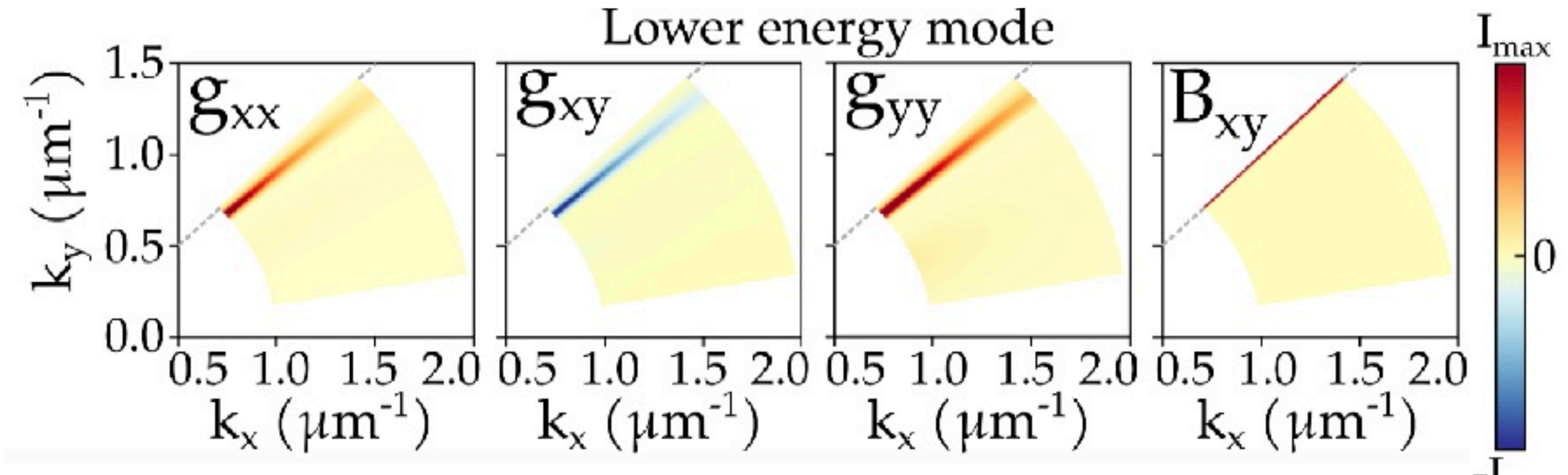

Cuerda et al., *Phys. Rev. Research* **6**, L022020 (2024)

Optical Raman lattice

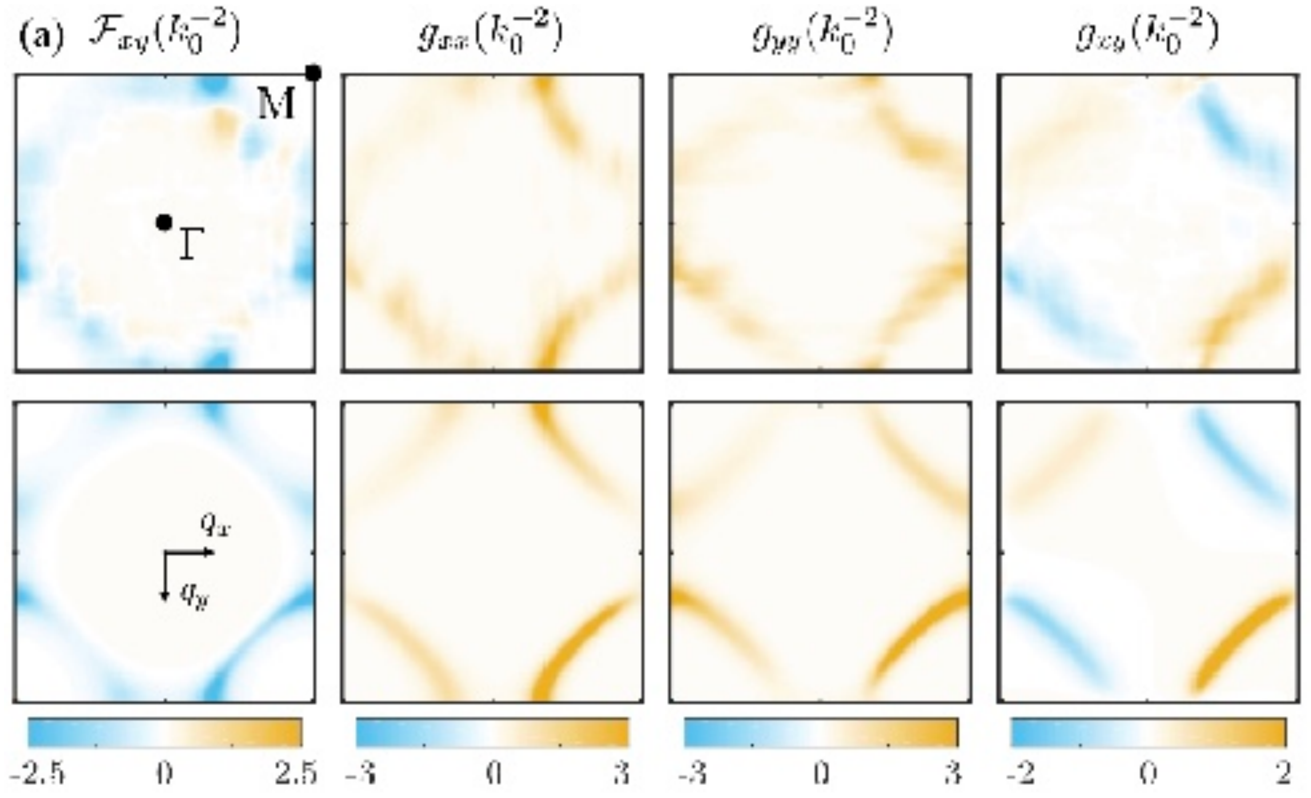

Chang-Rui et al., *Phys. Rev. Research* **5**, L032016 (2023)

The non-Hermitian Berry Curvature

Is there a bulk-radiation correspondence?

Yuan, GS et al., *Phys. Rev. Research* ***7****, 043141* (2025)

see also Yin et al. *Nat. Commun.* **16**, 2796 (2025)

Loss-designed lasing from BICs

R. Heilmann, G. Salerno, J. Cuerda, TK Hakala, and P. Törmä, *ACS Photonics* **9** 224 (2022)

G. Salerno, R. Heilmann, K. Arjas, K. Aronen, J.P. Martikainen, and P. Törmä, *Phys. Rev. Lett.* **129** 173901 (2022)

K. Arjas, J. M. Taskinen, R. Heilmann, G. Salerno and P. Törmä, *Nat. Commun.* **15**, *9544* (2024)

Aalto University

Research Council of Finland
MARIE CURIE ACTIONS

Plasmonic lattices

Surface Lattice Resonances in metallic nanoparticles arrays

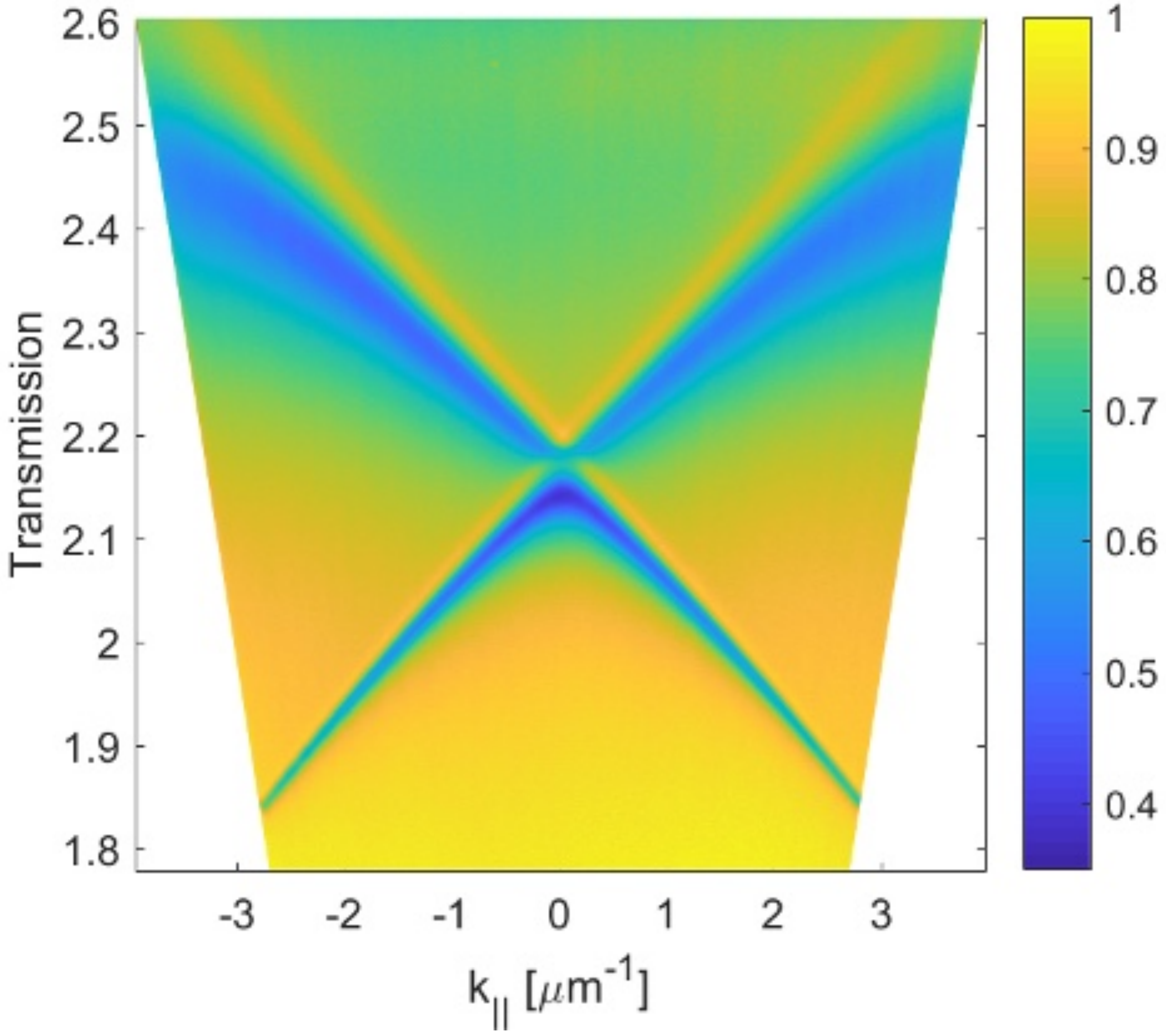

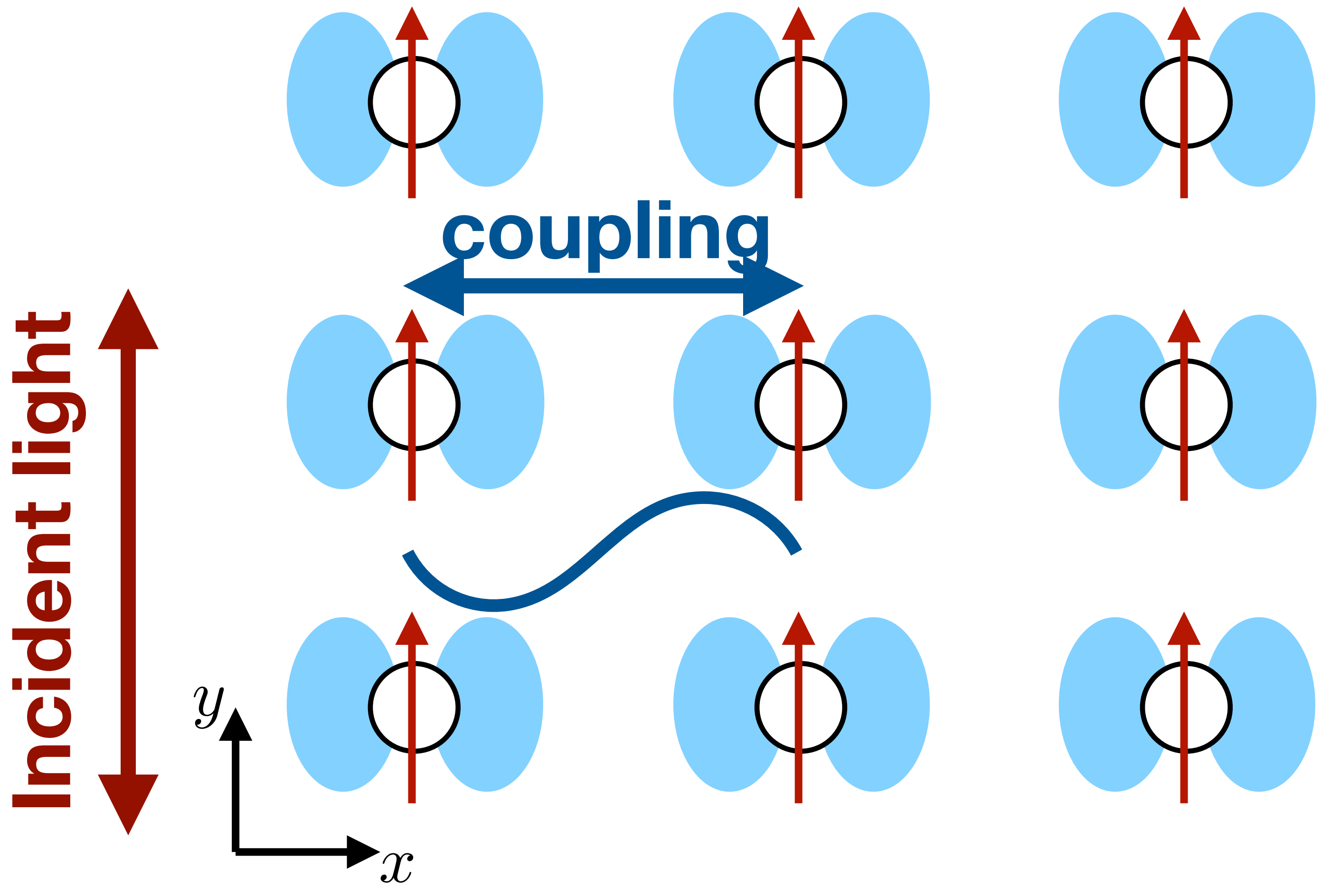

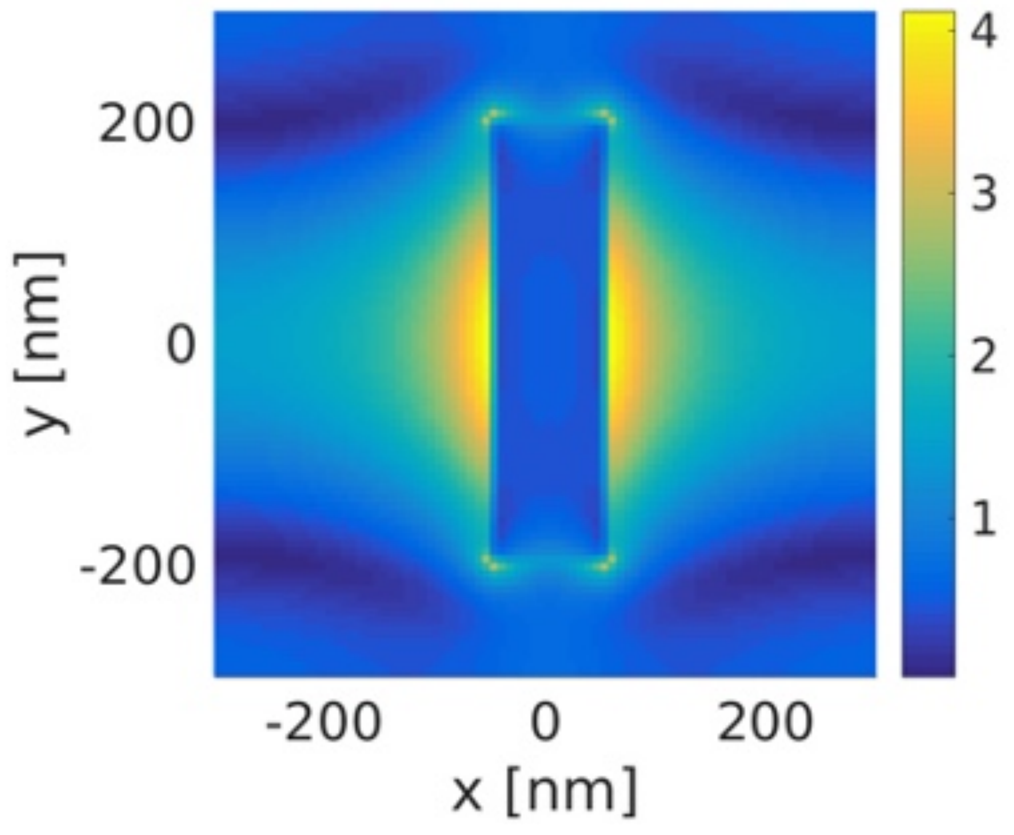

SLRs enable a strong confinement of light to the nanoscale!

Fluorescent dye molecules are used as a gain medium, and the system is optically pumped by a laser.

García de Abajo, *Rev. Mod. Phys.* **79**, 1267 (2007)
Tame *et al.*, *Nat. Phys.* **9**, 329 (2013)

Zhou *et al.*, *Prog. Quantum Electr.* **65**, 1 (2019)
Bozhevolnyi, Martin-Moreno & Garcia-Vidal, eds. *Quantum plasmonics*

A quadrumer array

Modes of a C4-symmetric system (FEM)

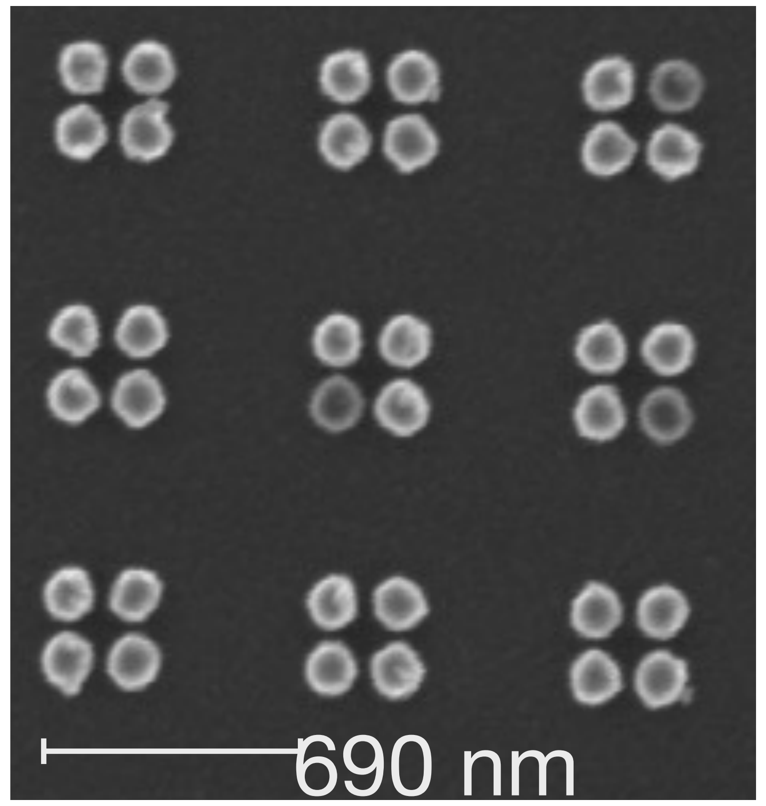

C_4	A	0
	B	π
	E^*	$\pi/2$

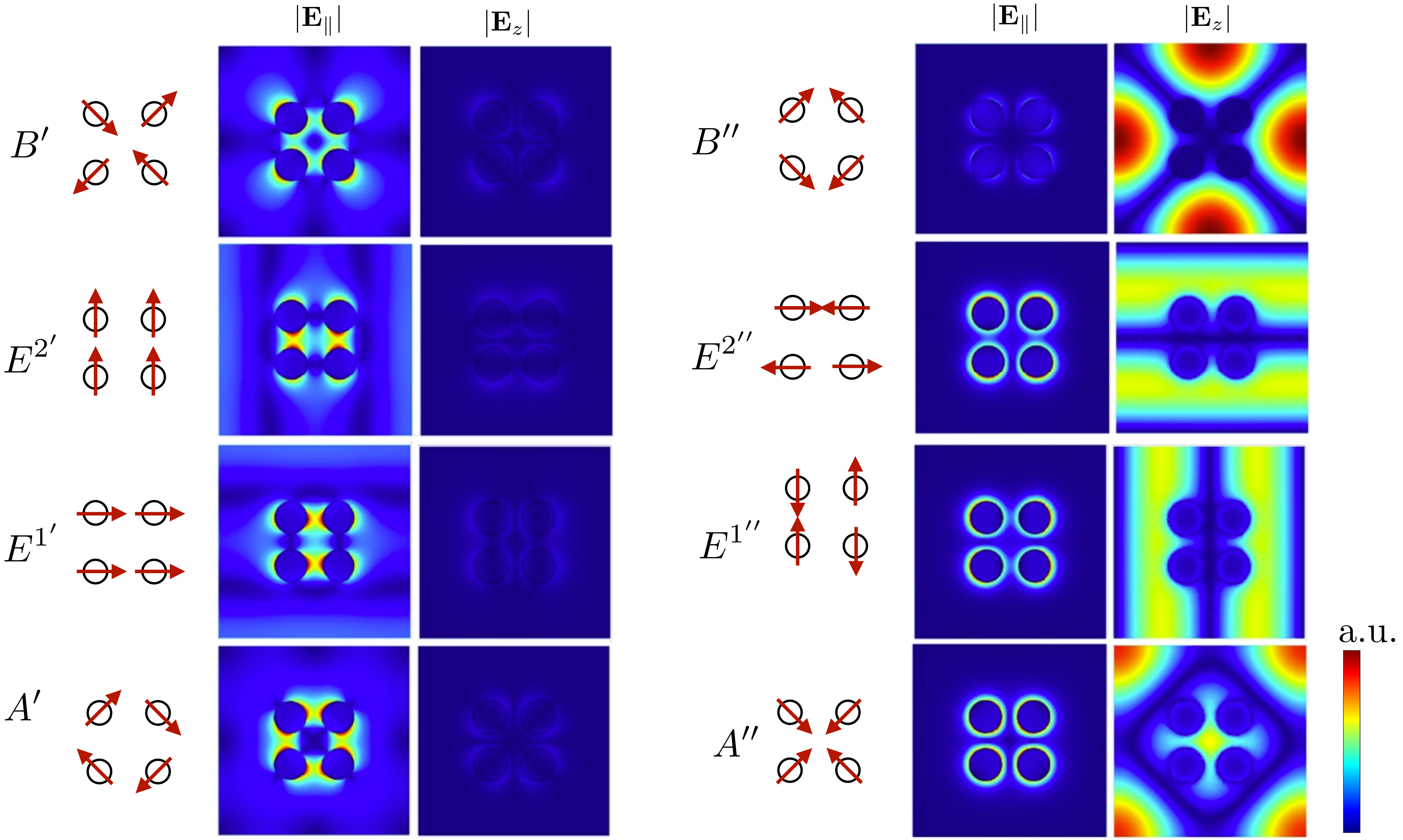

Finite Element Methods simulations

Heilmann, GS et al. *ACS Photonics* **9**, 224 (2022)

A quadrumer array

The experimental signatures of lasing

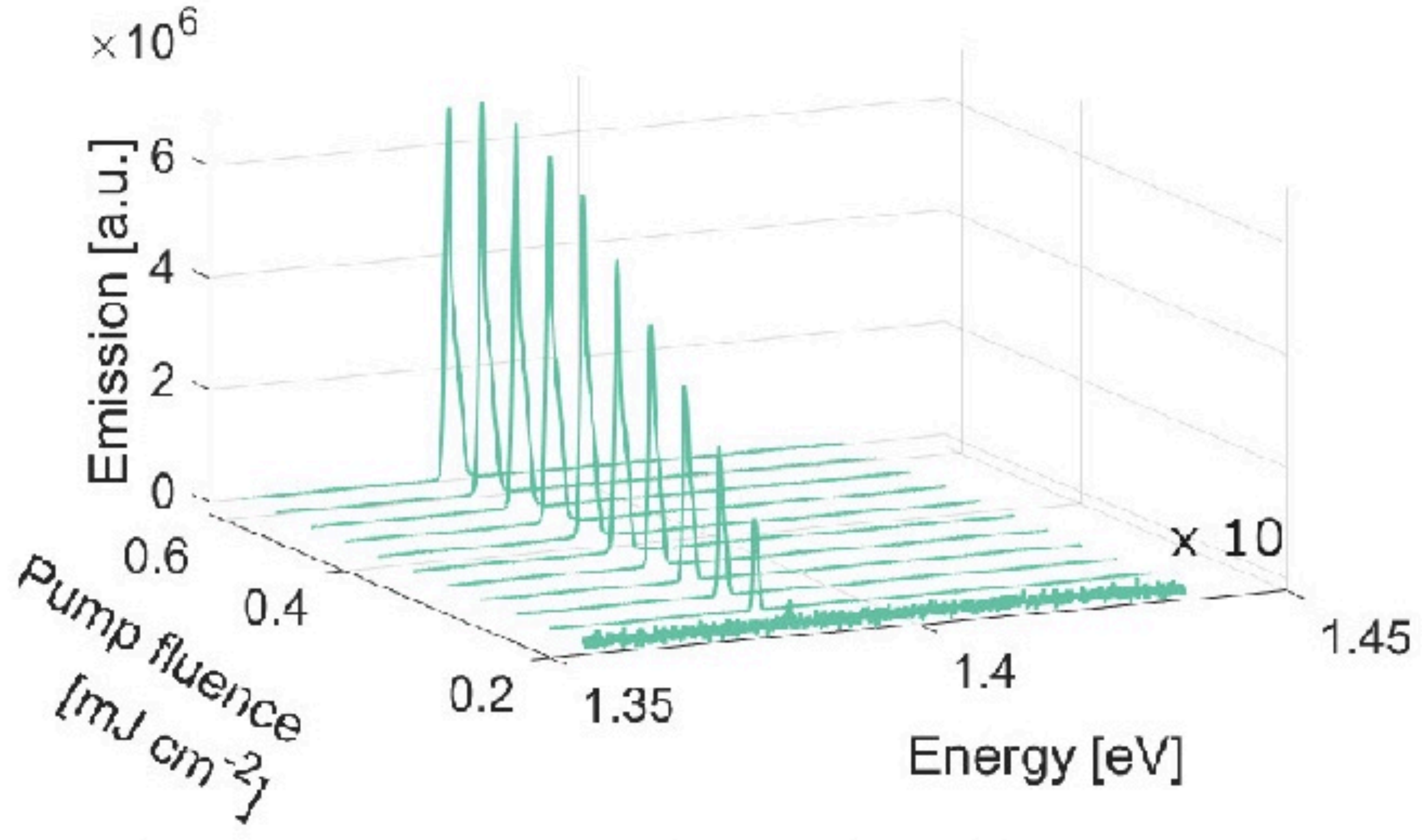

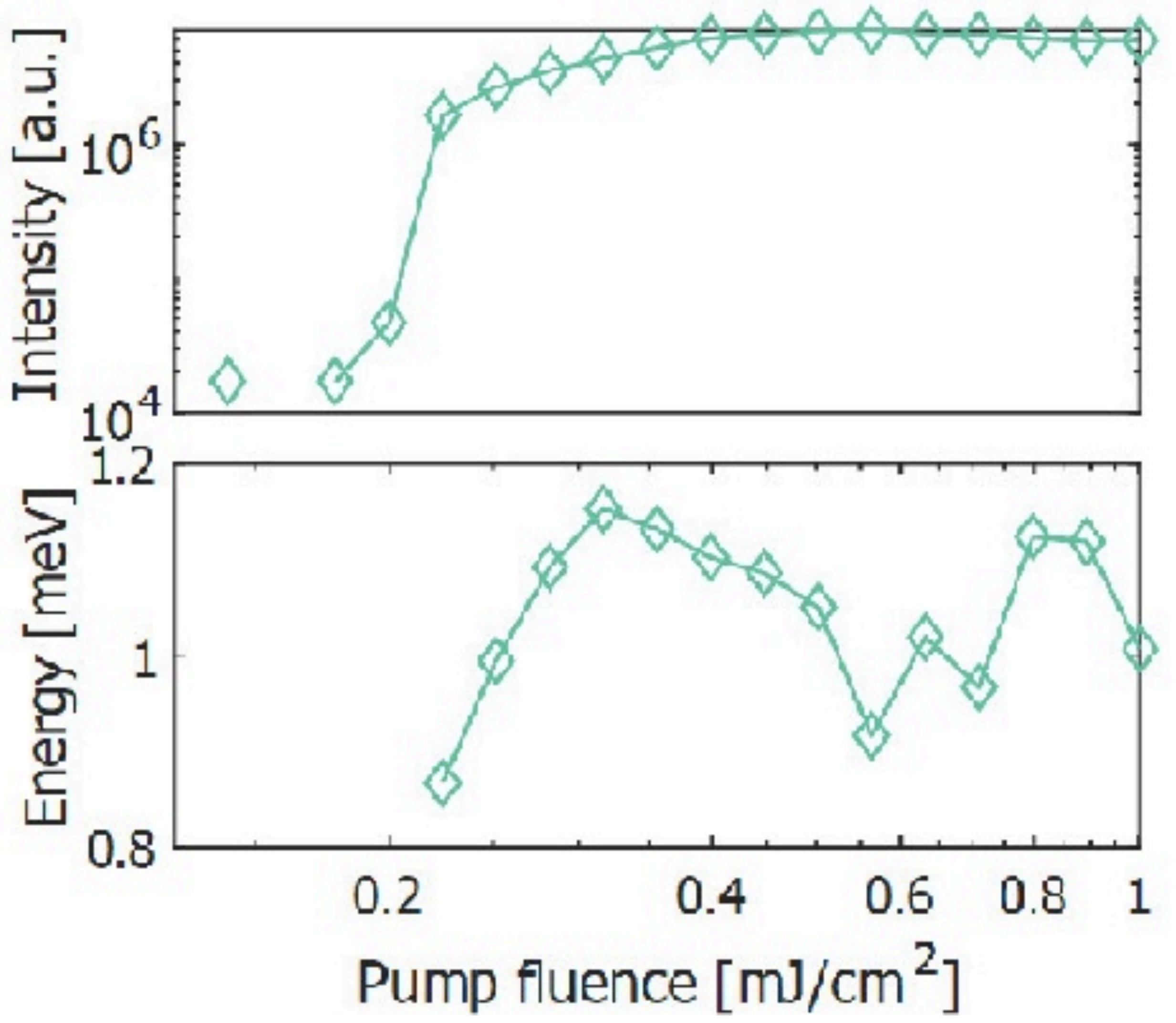

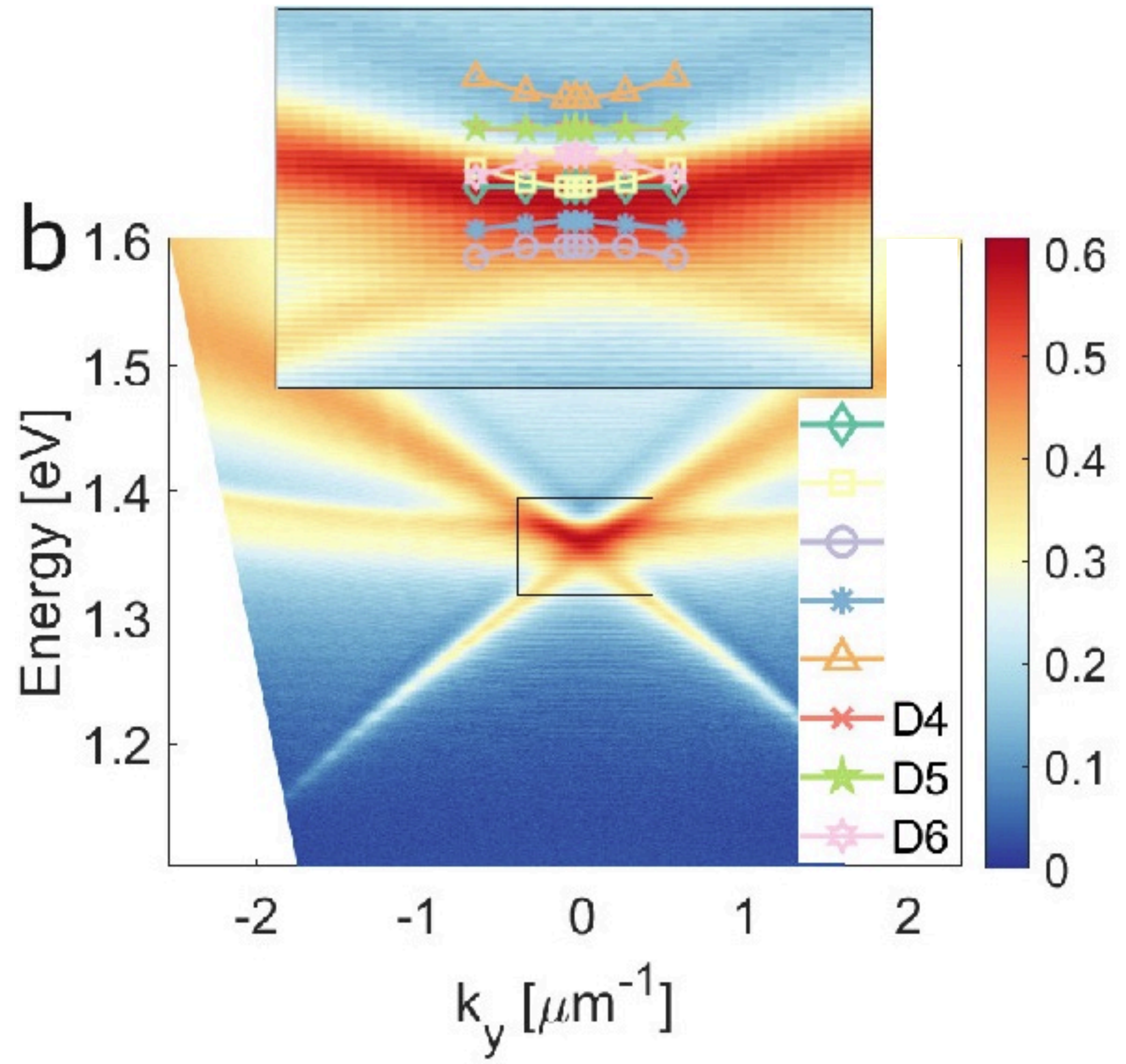

Lasing energy = 1.382 eV
Linewidth = 1 meV
Q-factor = 1382

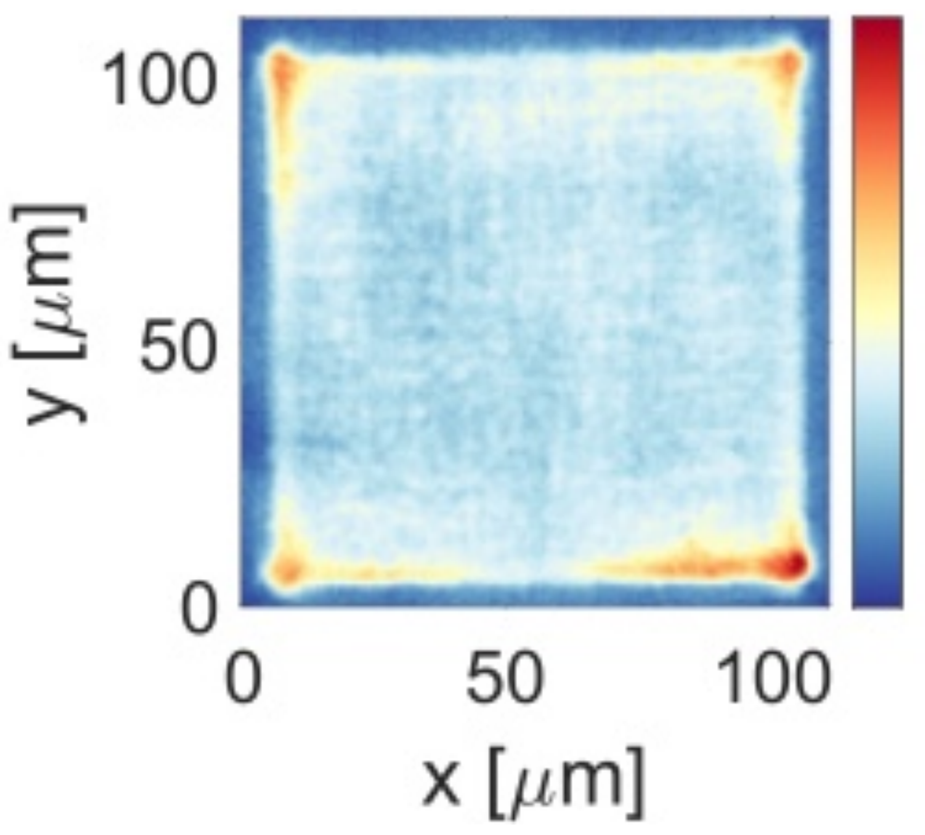

How to identify which mode is lasing?

Heilmann, GS et al. *ACS Photonics* **9**, 224 (2022)

A quadrumer array
Polarization vortex in real space

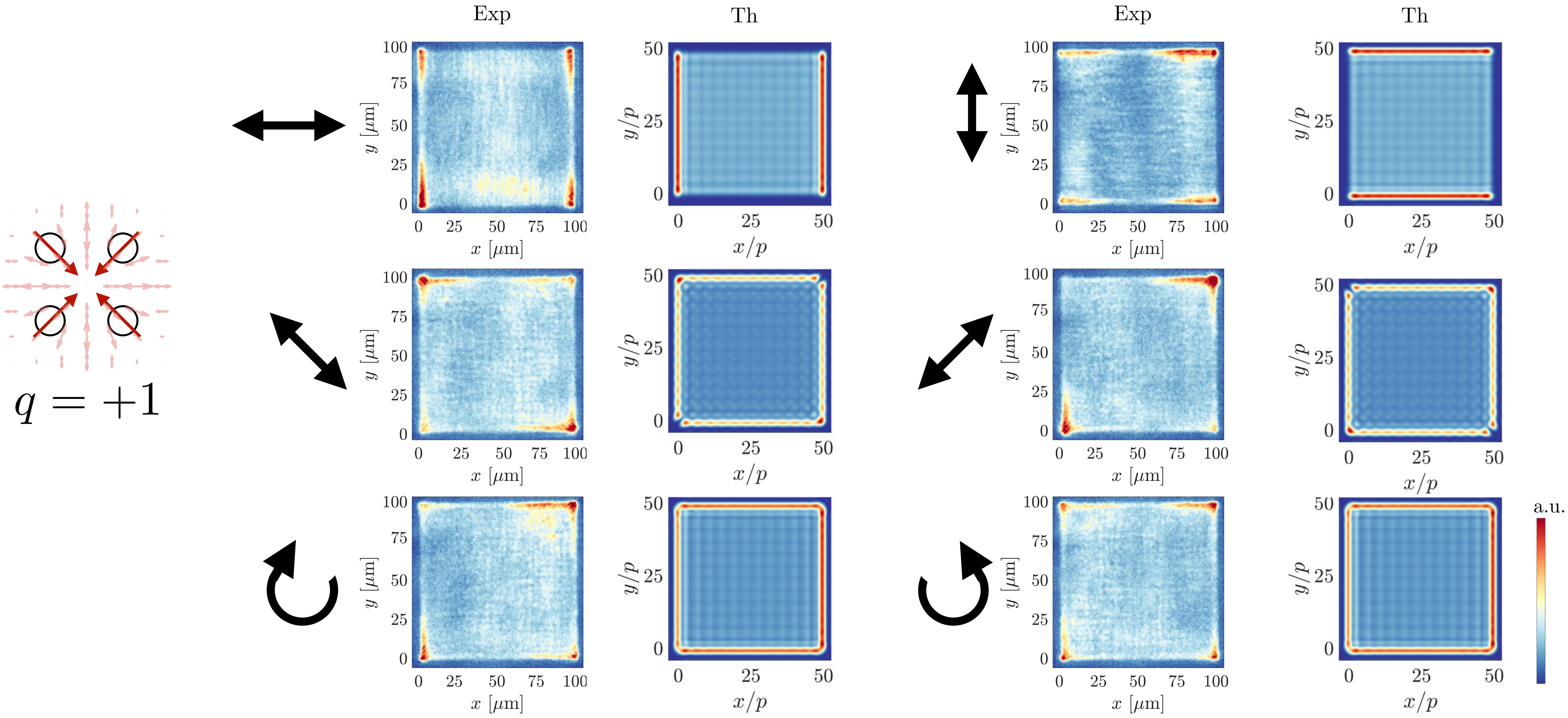

The boundaries provide a leak channel to observe the BIC.

Heilmann, GS et al. *ACS Photonics* **9**, 224 (2022)

A hexamer array

Lasing mode transition

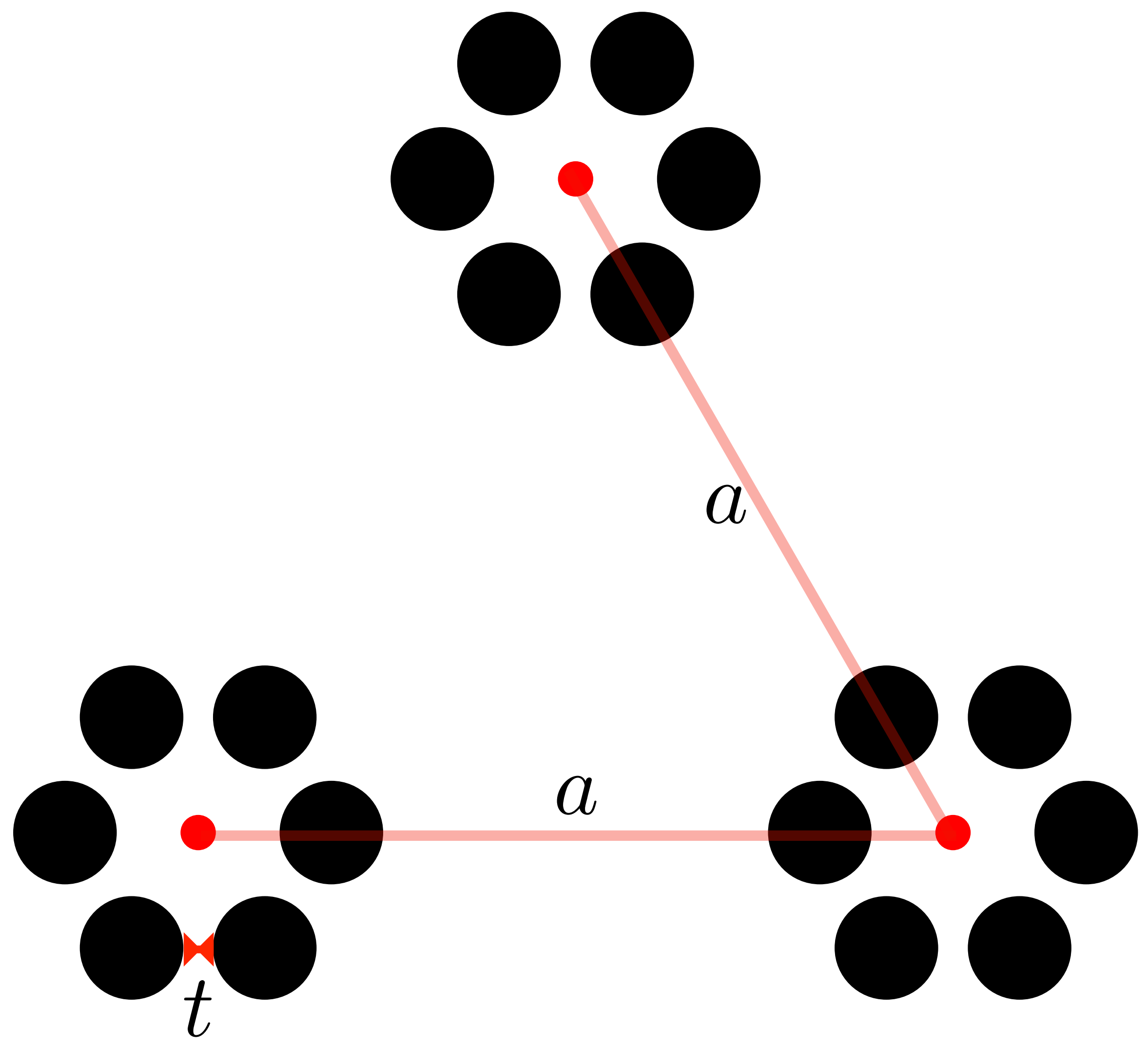

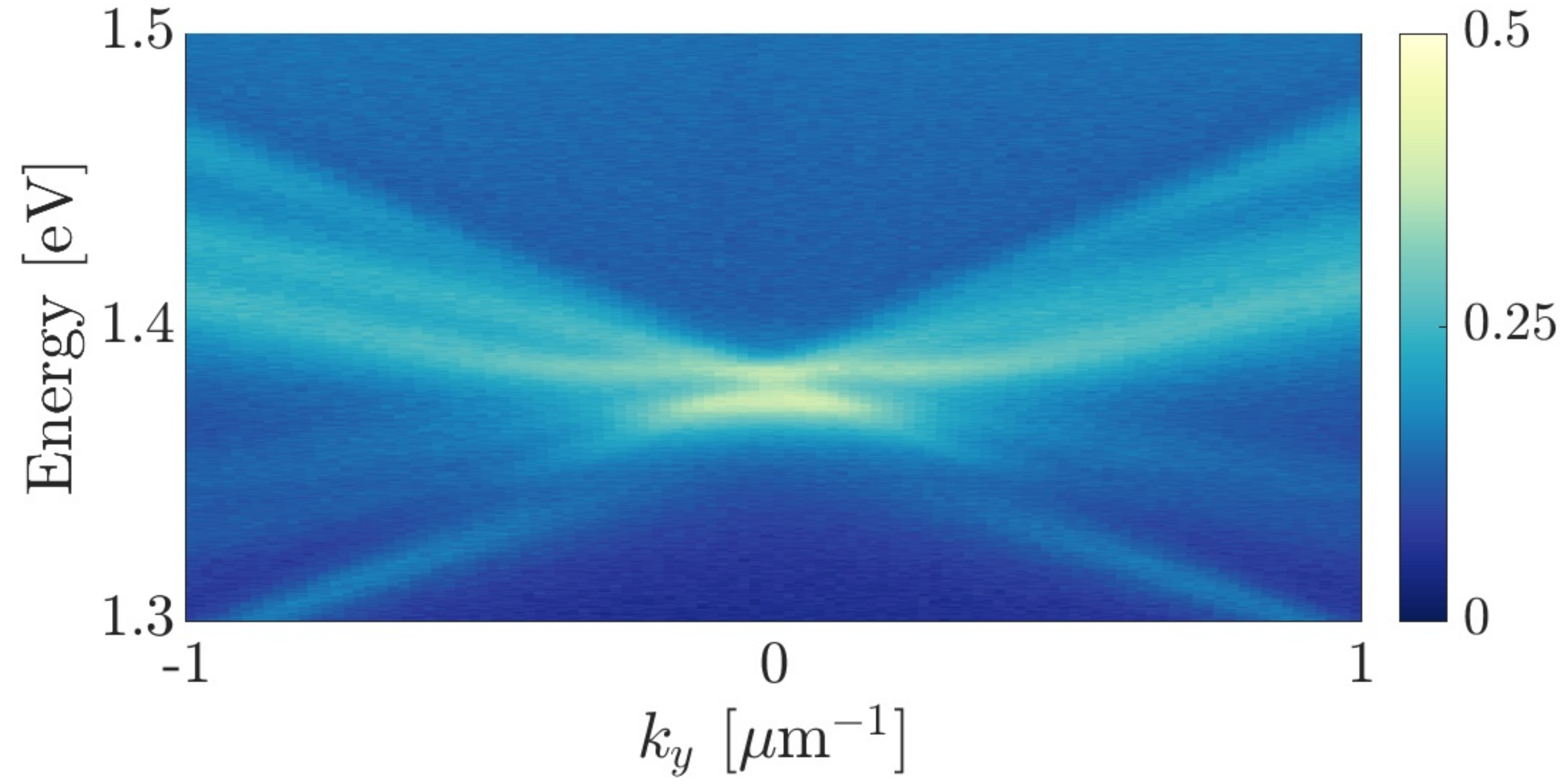

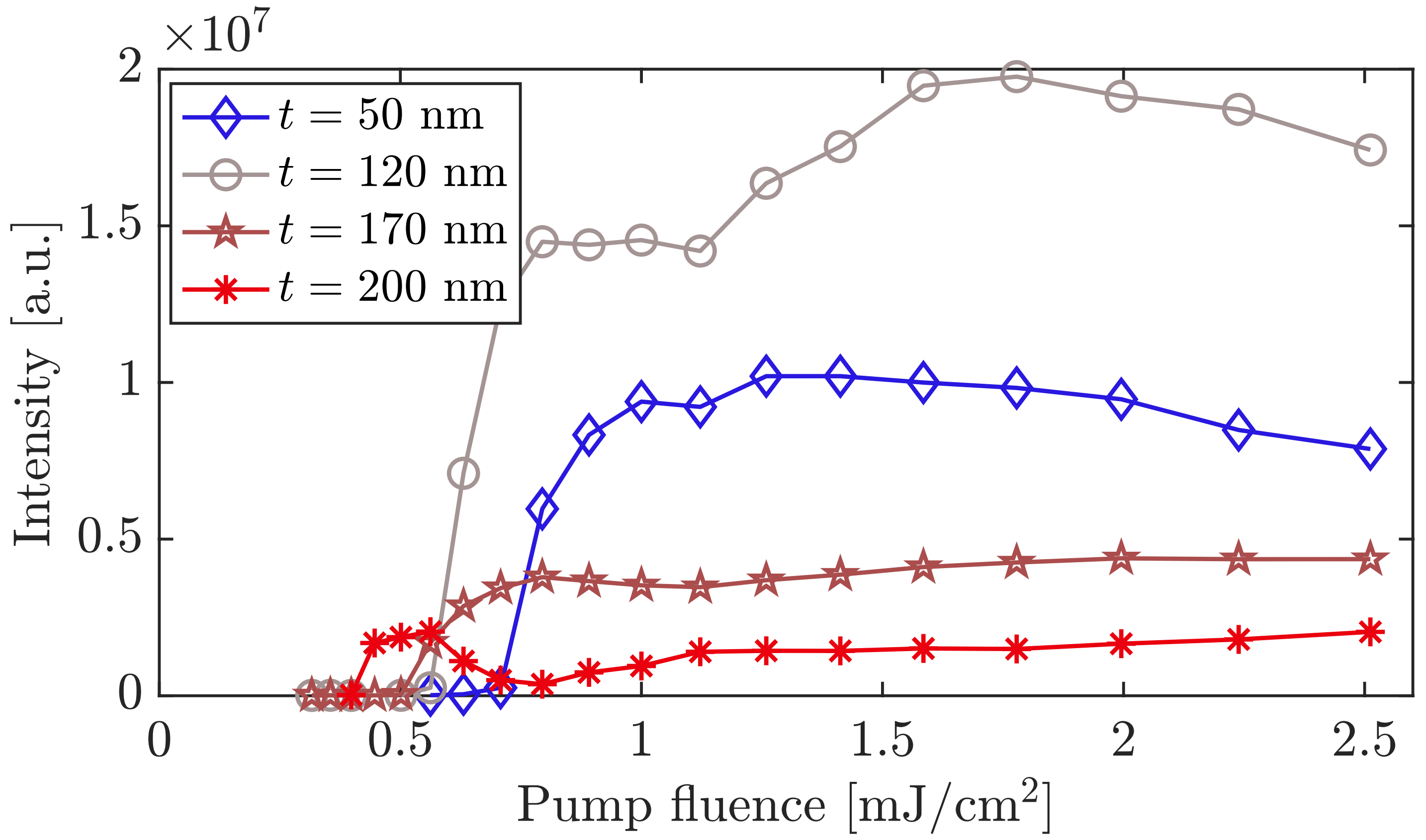

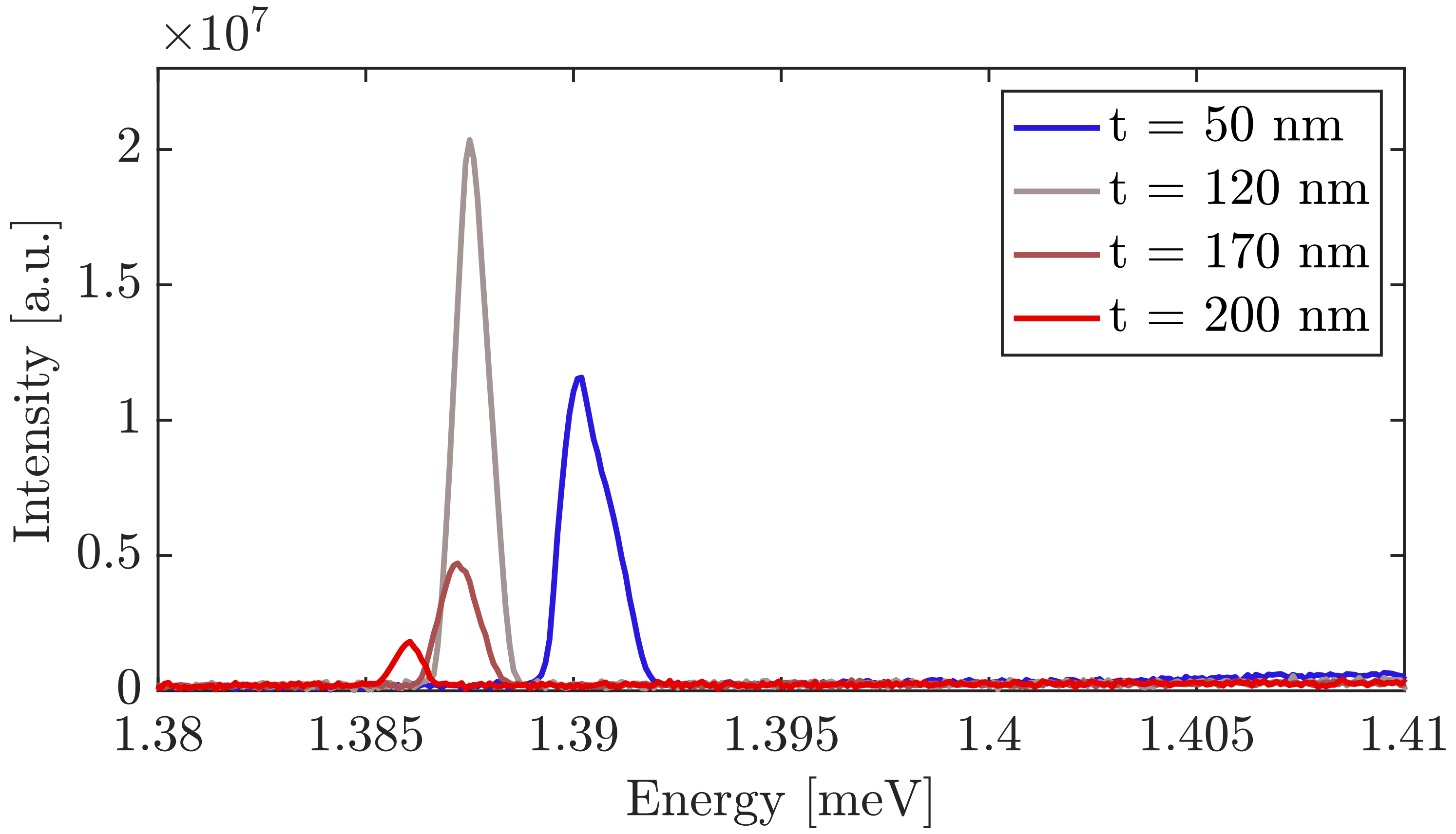

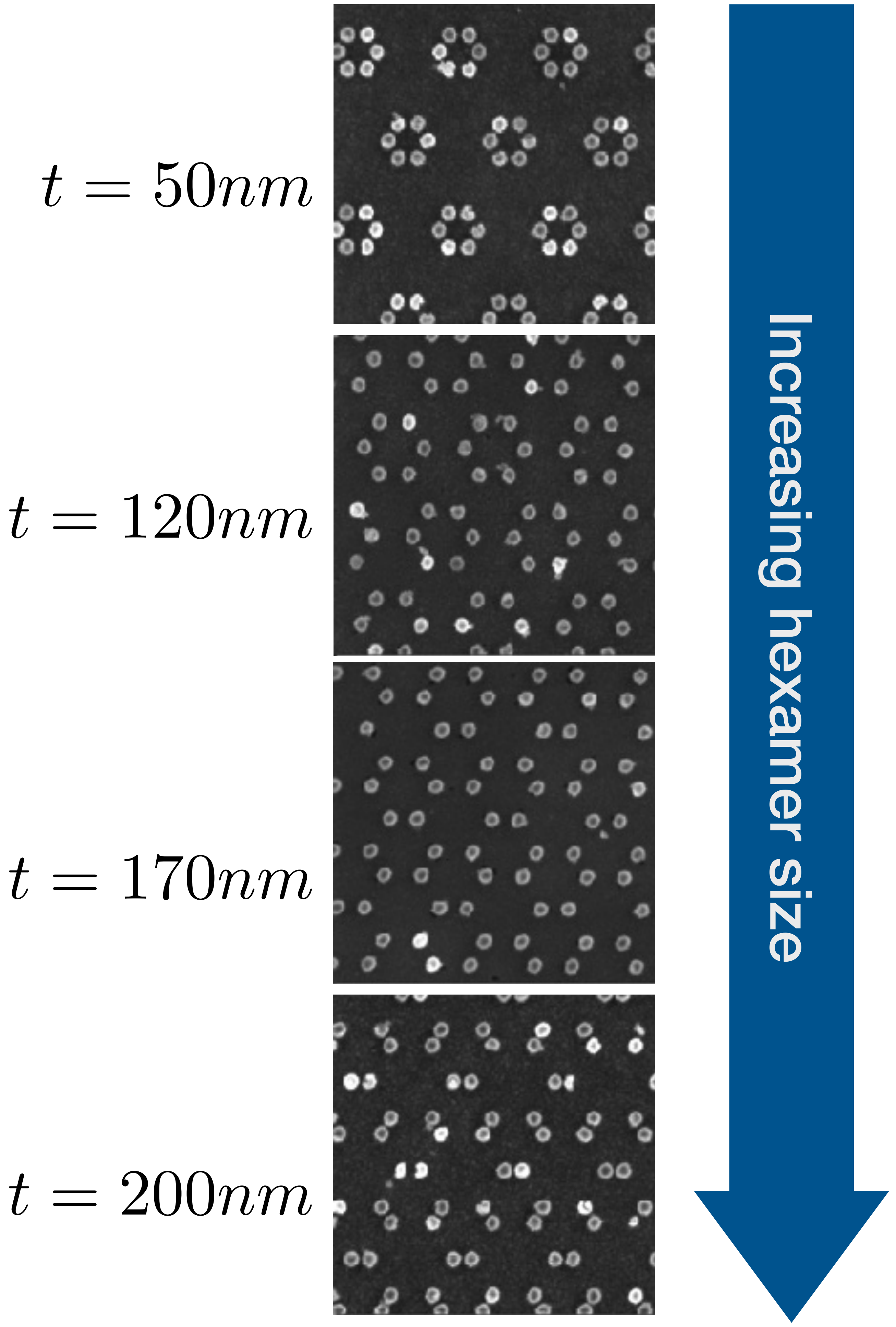

GS et al., *Phys. Rev. Lett.* **129**, 173901 (2022)

A hexamer array

The modes and their momentum space polarization properties

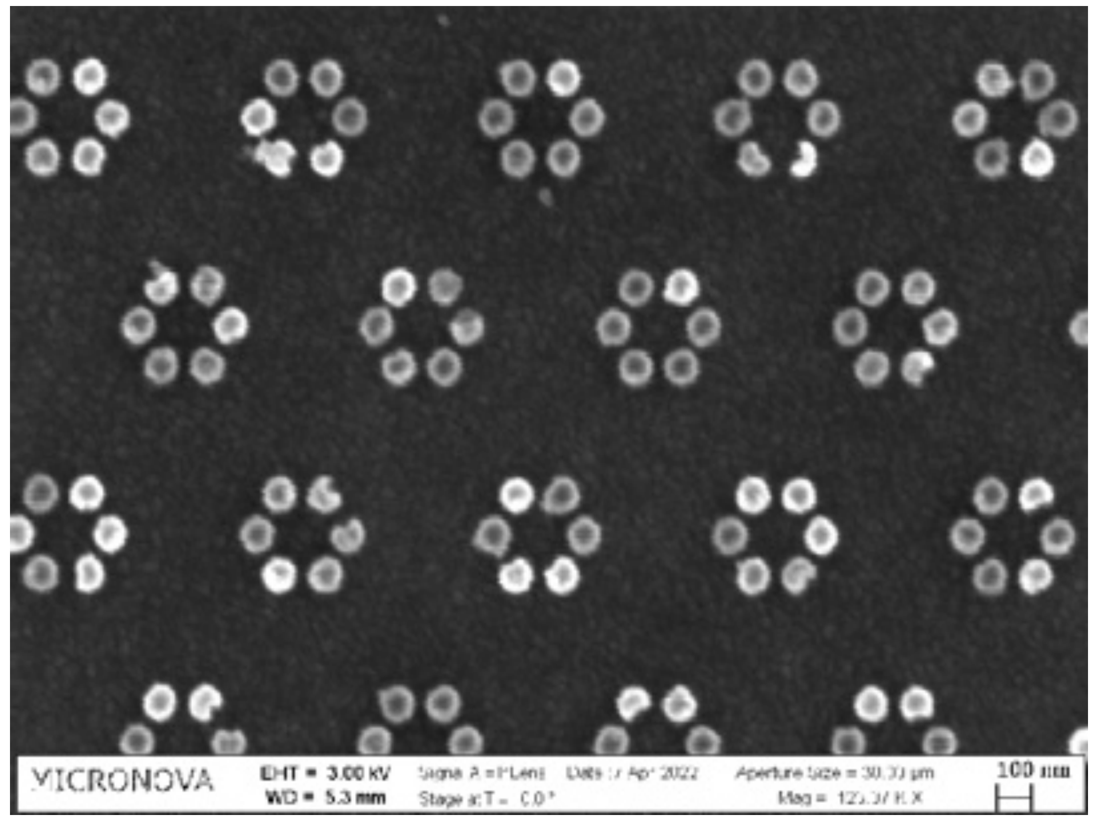

C_6	A	0	$+1$
	B	π	-2
	E_1^*	$\pi/3$	0
	E_2^*	$2\pi/3$	-1

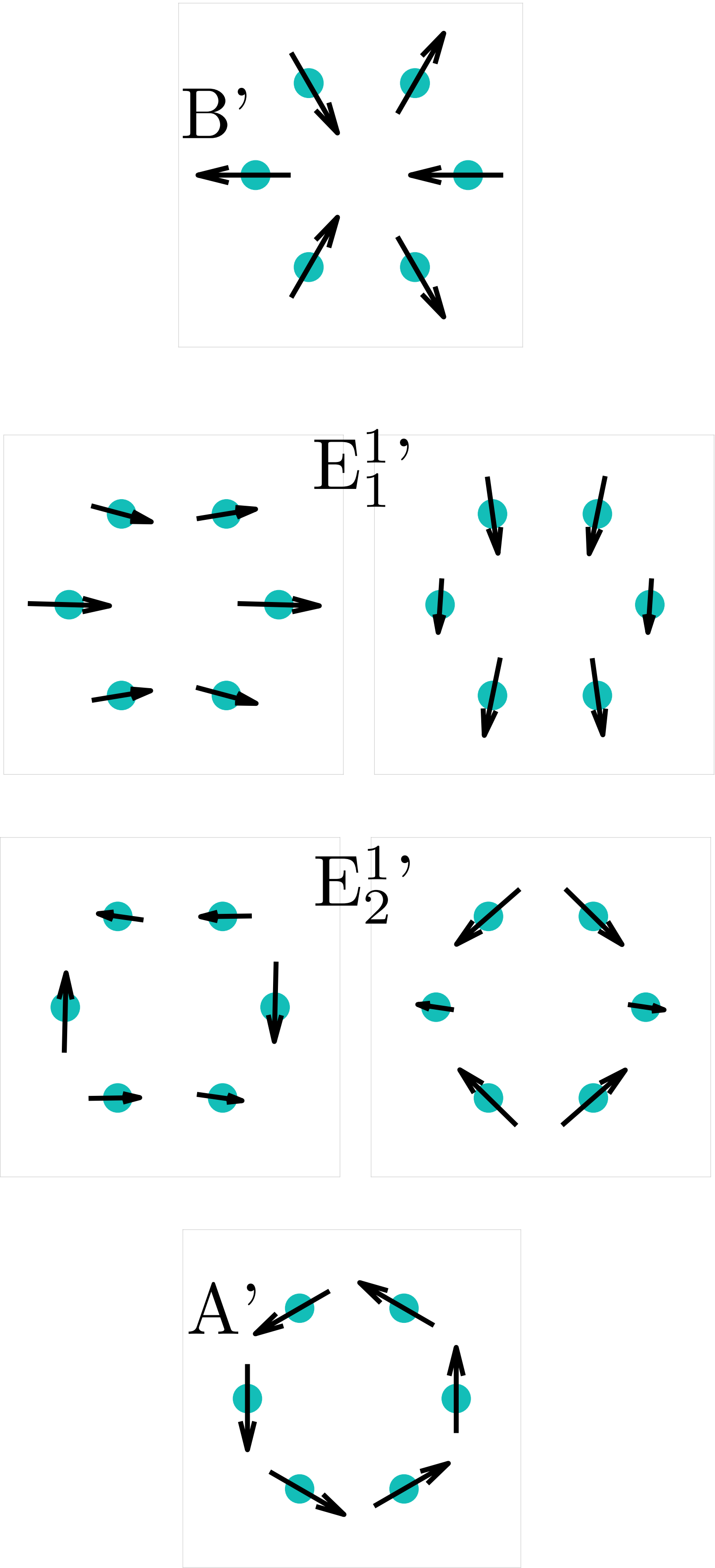

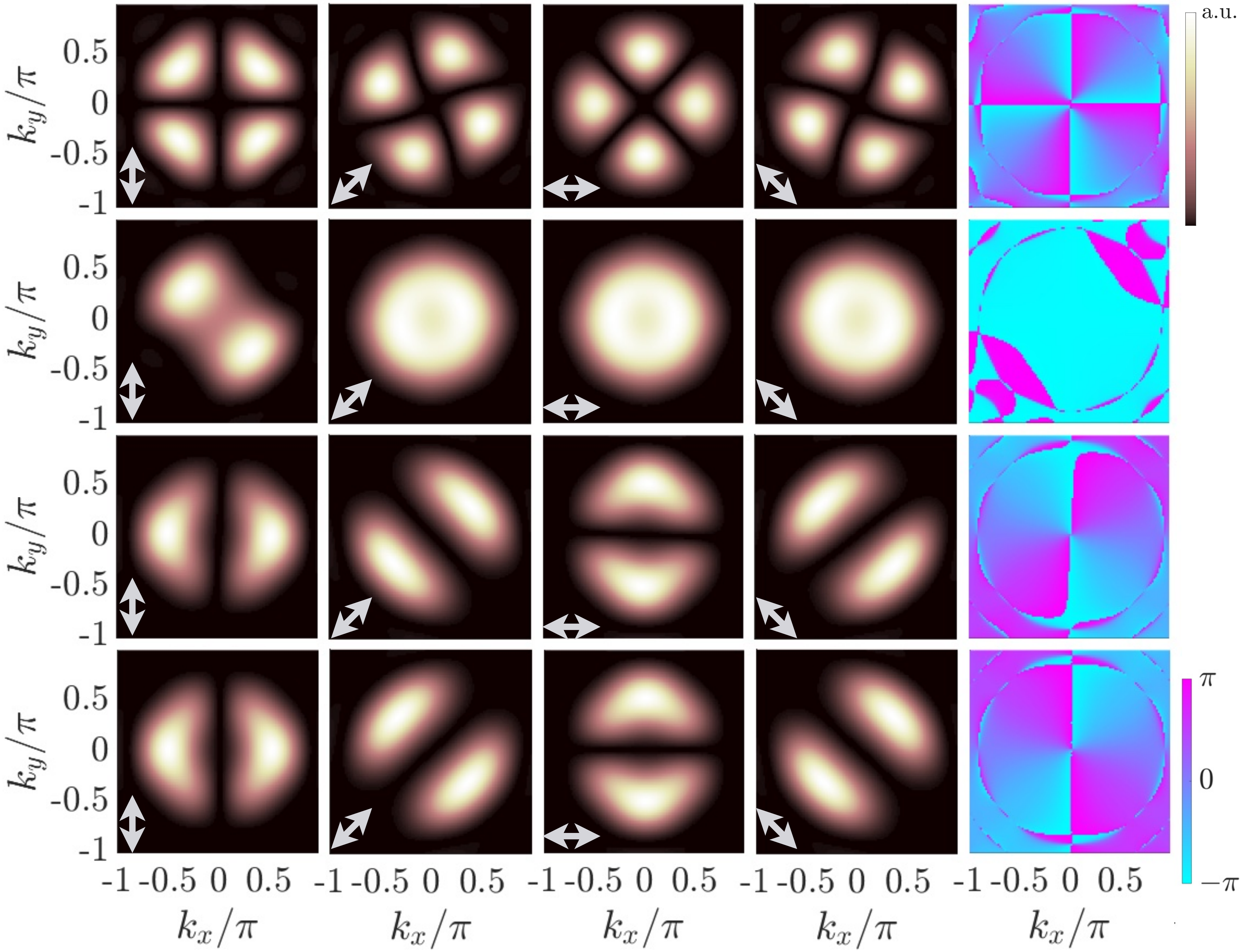

GS et al., *Phys. Rev. Lett.* **129**, 173901 (2022)

A hexamer array

Polarization-resolved measurement in momentum space

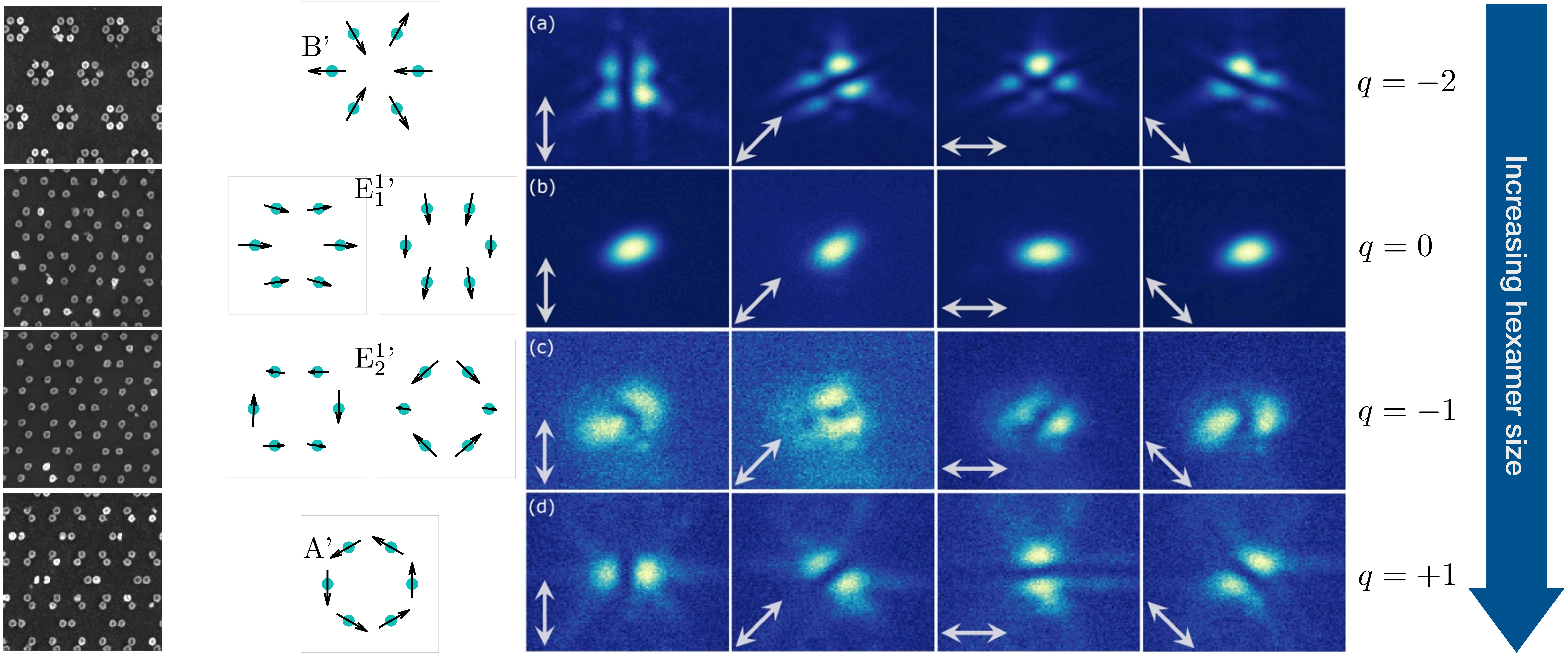

GS et al., *Phys. Rev. Lett.* **129**, 173901 (2022)

A hexamer array

A “loss induced” transition

- The mode with the highest Q-factor is usually preferred for lasing.

- T-matrix calculations show that this transition is attributed to a change of the modes’ losses when the unit cell is varied.

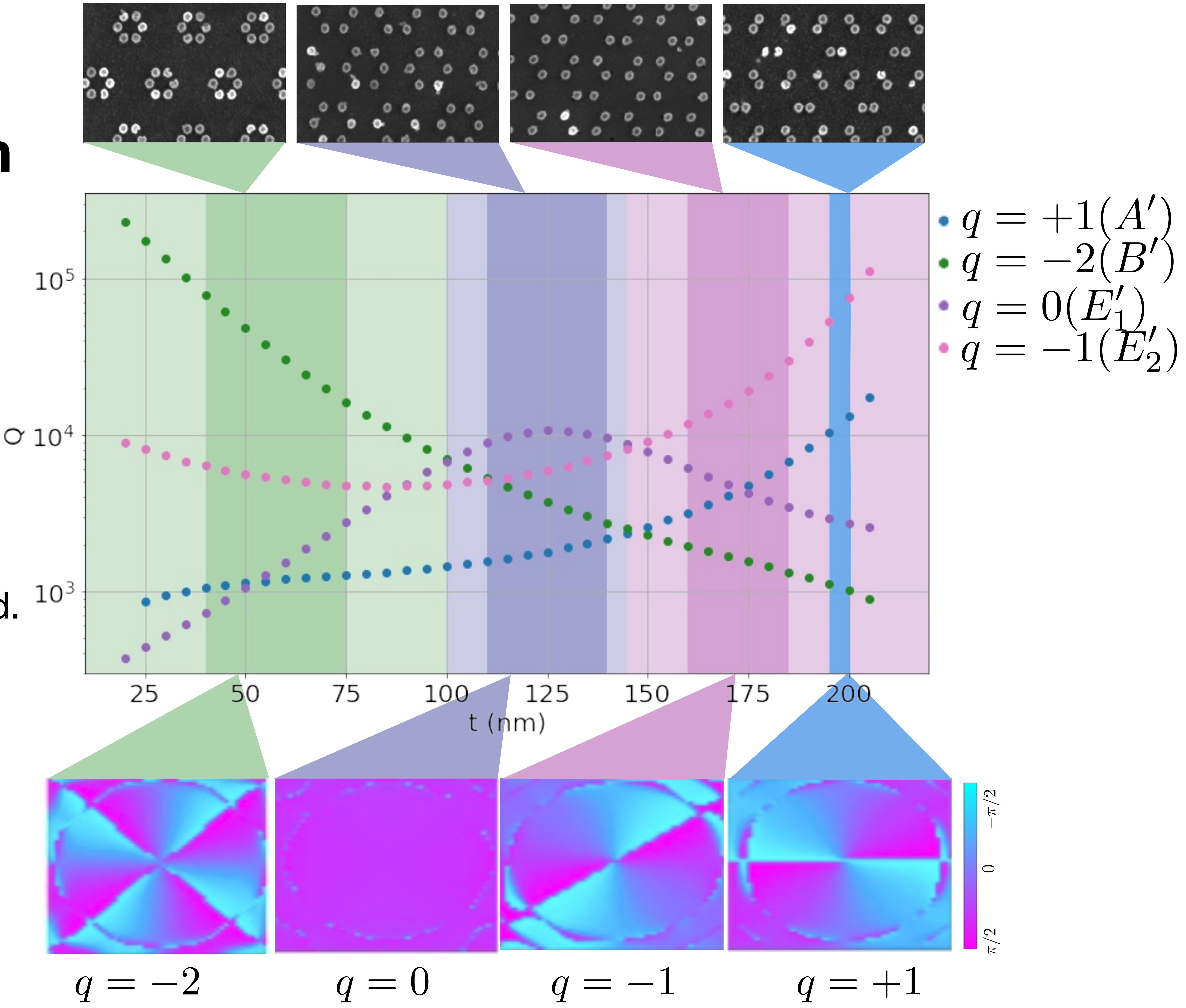

GS et al., *Phys. Rev. Lett.* **129**, 173901 (2022)

A hexamer array

A “loss induced” transition

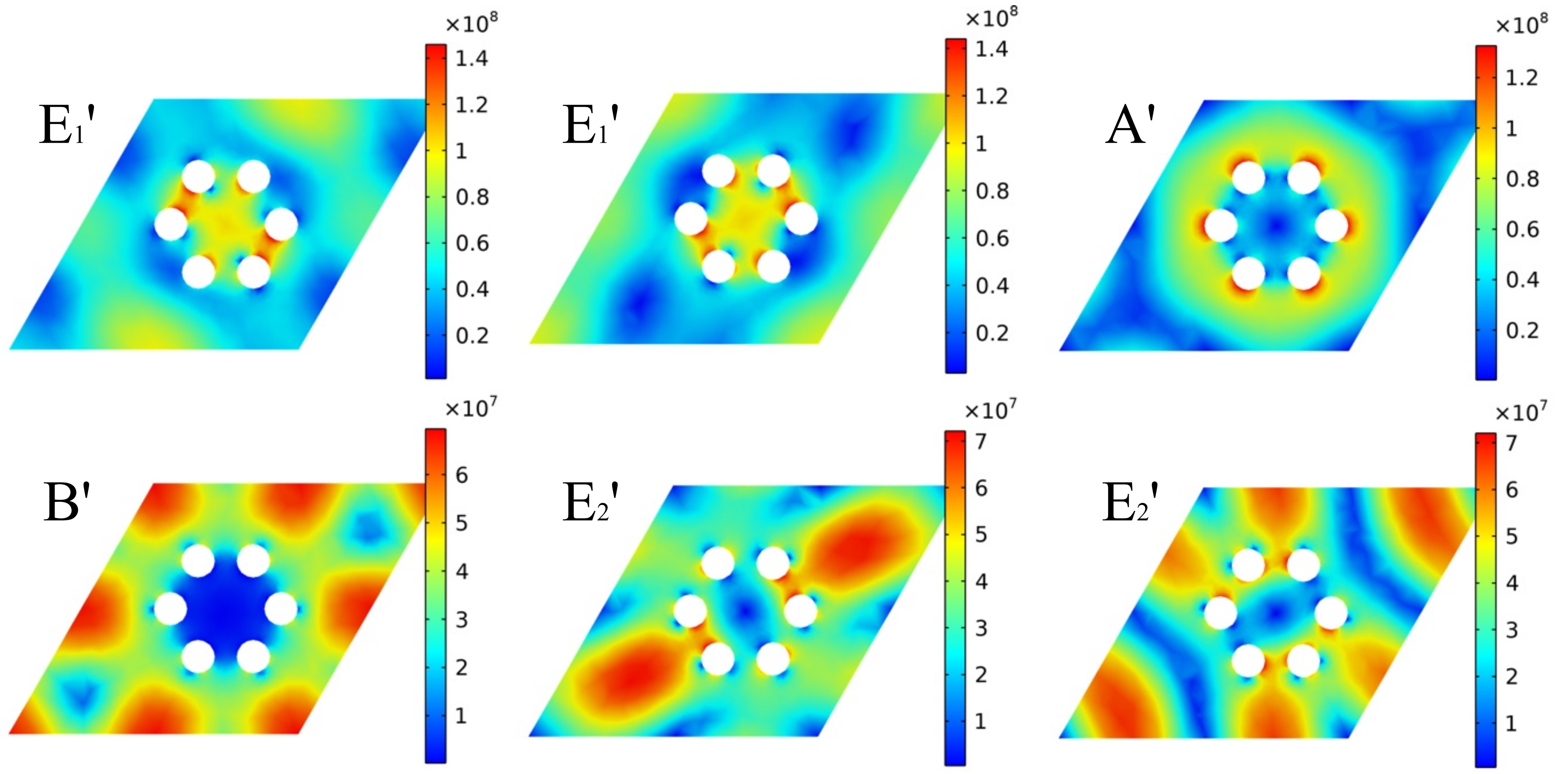

Modes for t = 50nm (lasing B’)

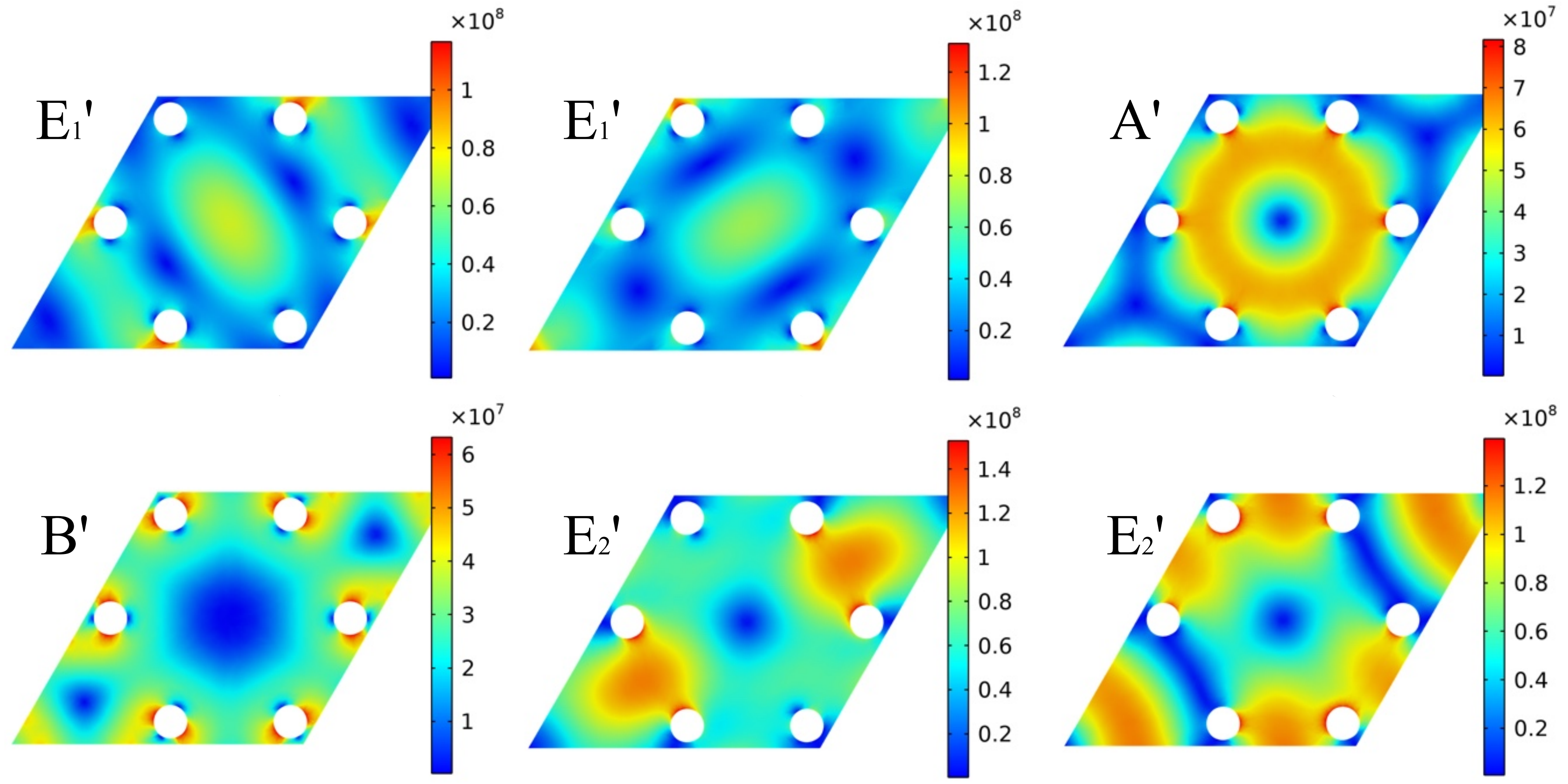

Modes for t = 200nm (lasing A’)

- Finite Element simulations of the field distribution inside the unit cell.
- Despite the symmetry of the modes being the same, the Electric-field hotspots are closer to the nanoparticles for high-lossy modes (Ohmic losses).
- Mode competition for lasing will depend on spatial overlap of the Electric-field with the gain.

GS et al., *Phys. Rev. Lett.* **129**, 173901 (2022)

A quasicrystal with C_{12} symmetry

Design by symmetry of the lasing mode

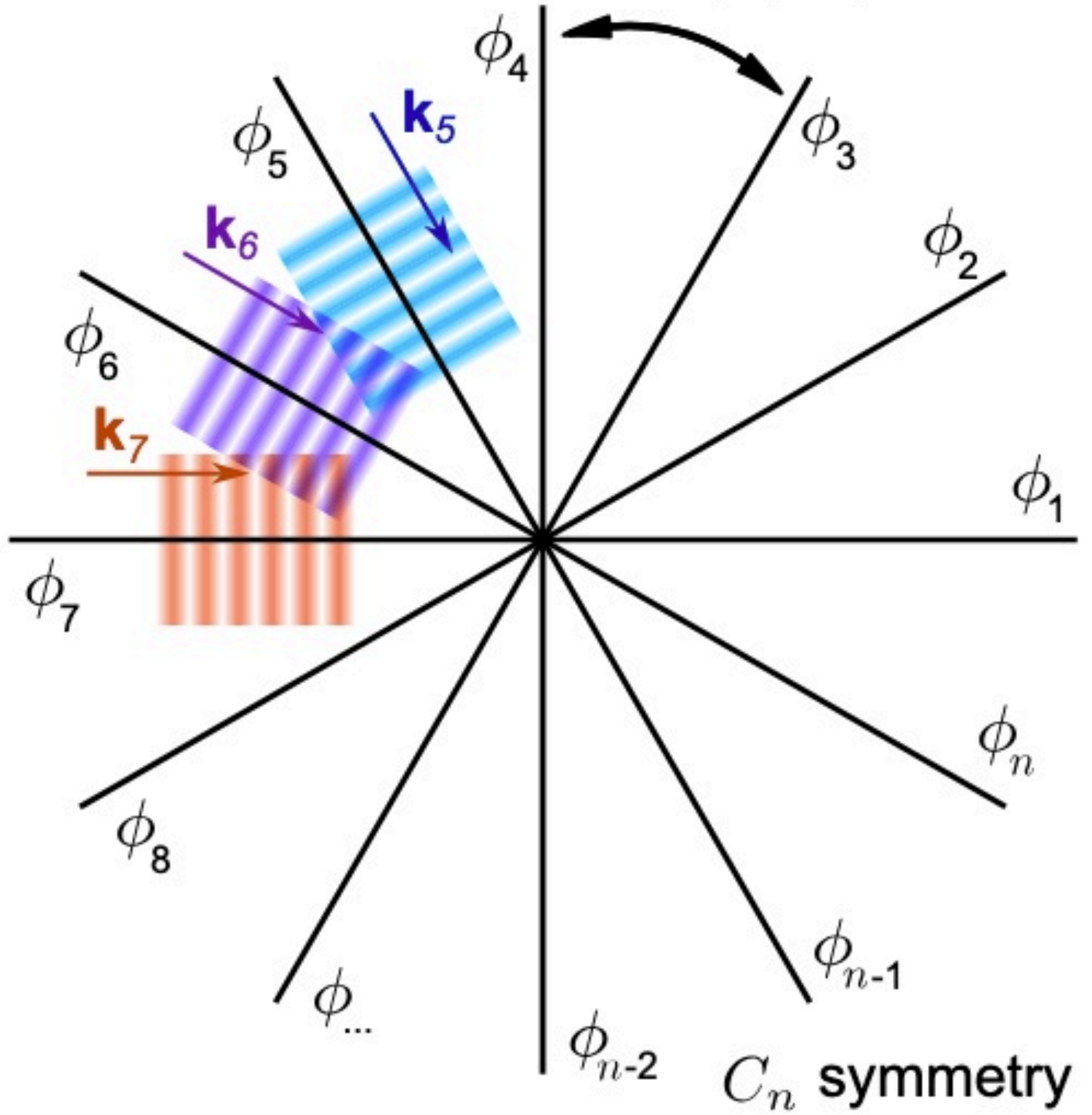

Topological charge

$$q_{\mathrm{IR}} = 1 - \frac{n}{2\pi}\arg(\epsilon_{\mathrm{IR}}) + n \cdot m, \quad m \in \mathbb{Z}$$

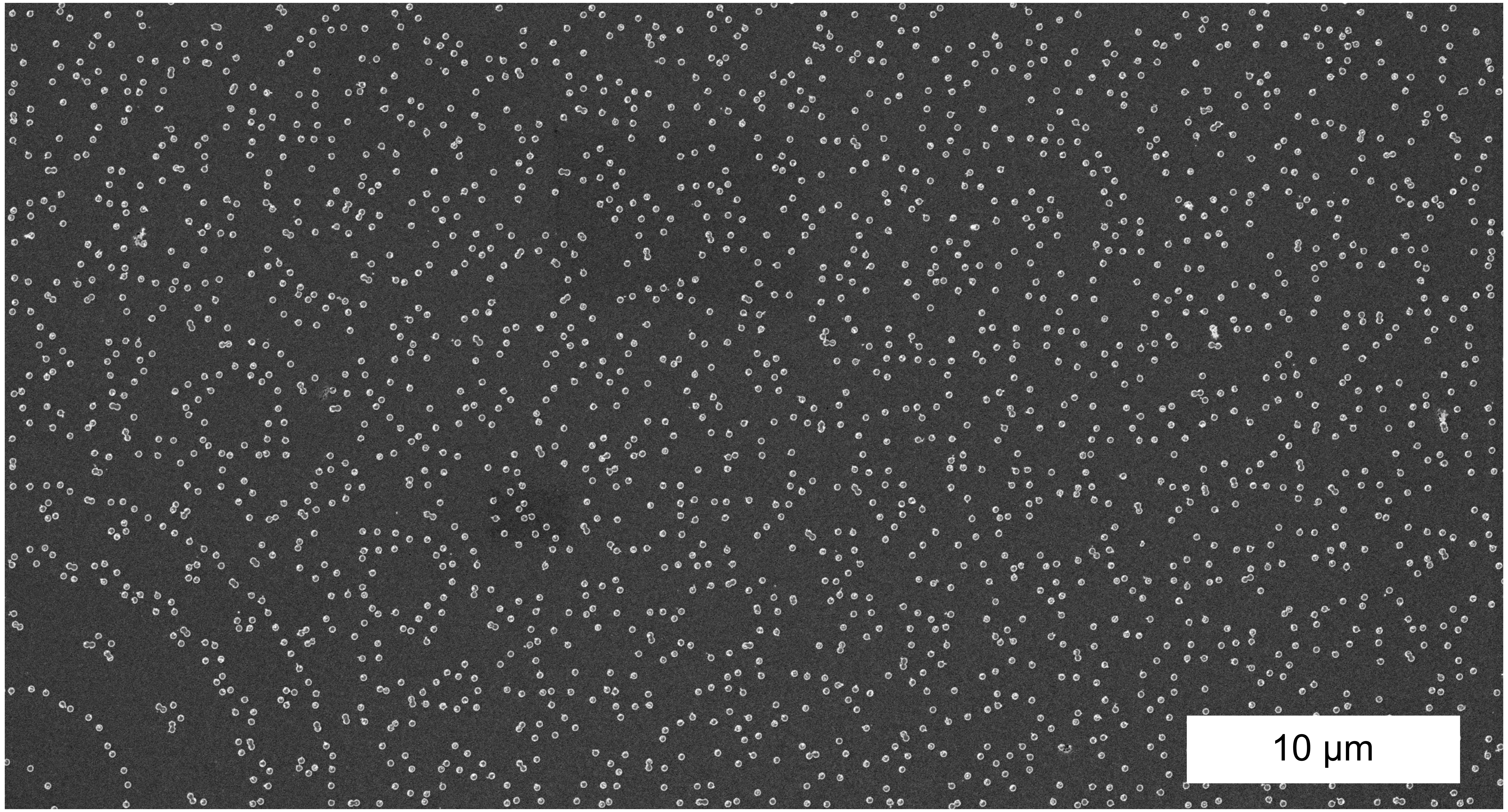

Arjas, GS et al., *Nat. Commun.* **15**, 9544 (2024)

A quasicrystal with C_{12} symmetry

The structure factors

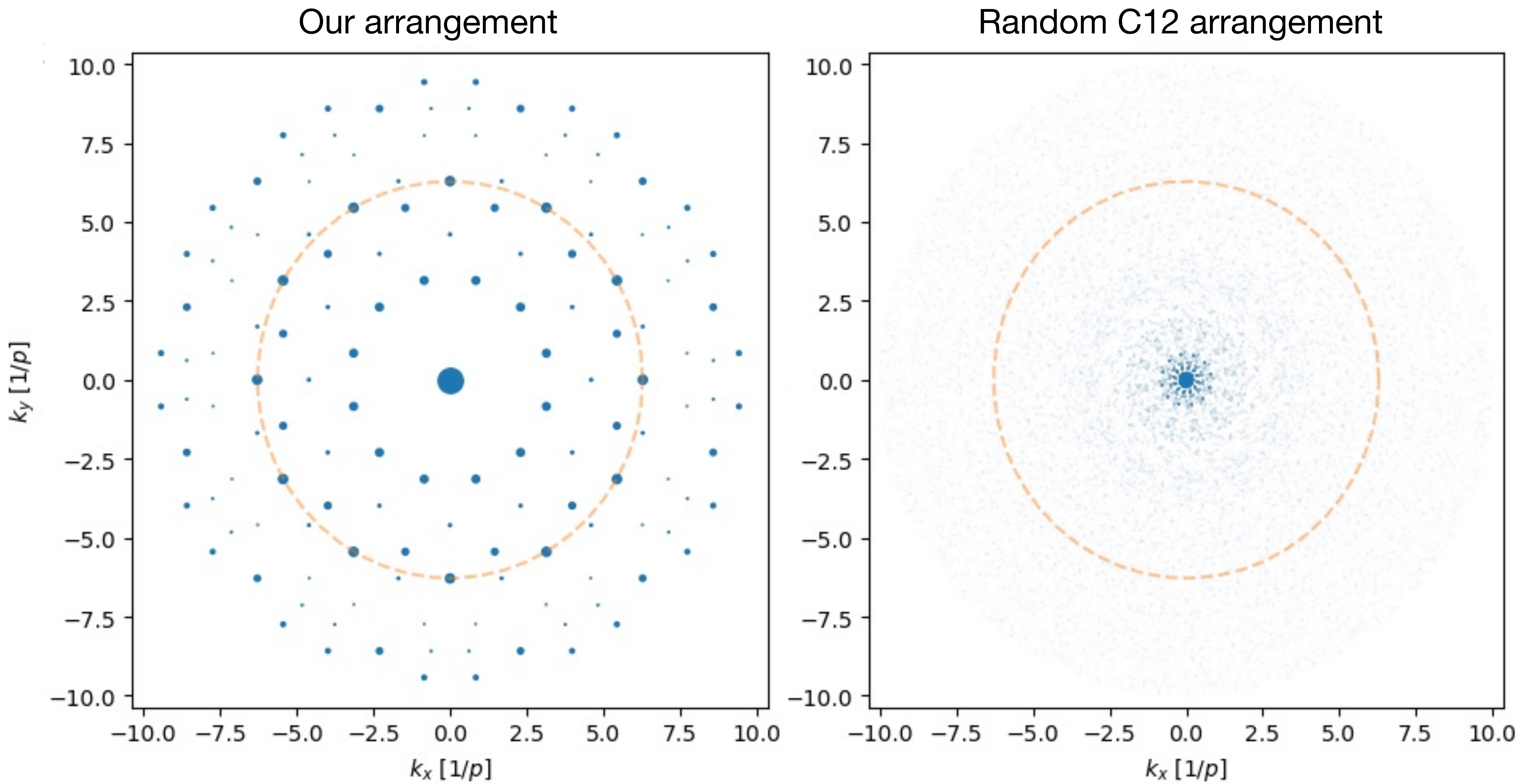

Arjas, GS et al., *Nat. Commun.* **15**, 9544 (2024)

A quasicrystal with C_{12} symmetry

High topological charges in lasing

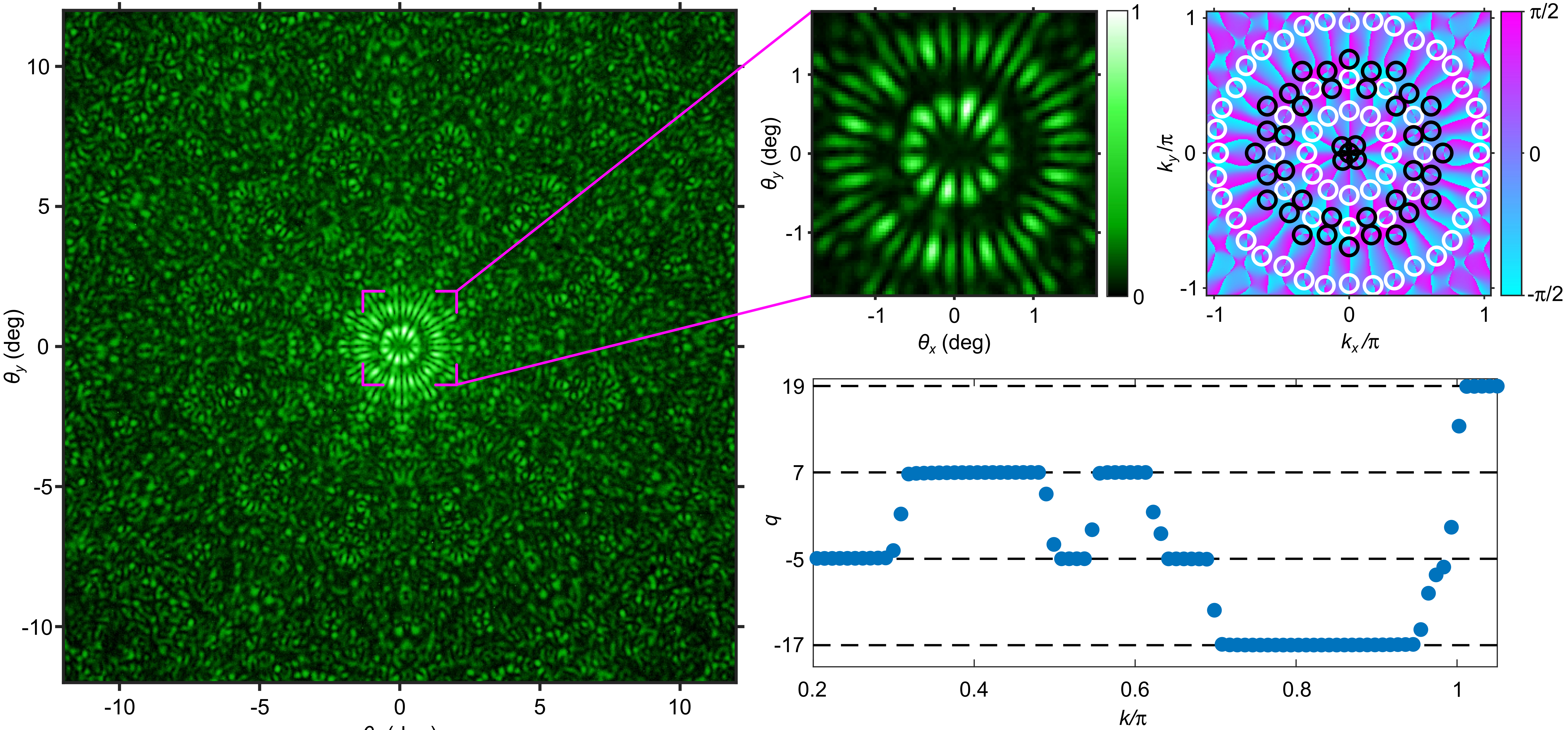

Arjas, GS et al., *Nat. Commun.* **15**, 9544 (2024)

A quasicrystal with C_{12} symmetry

Polarization resolved measurements and theory comparison

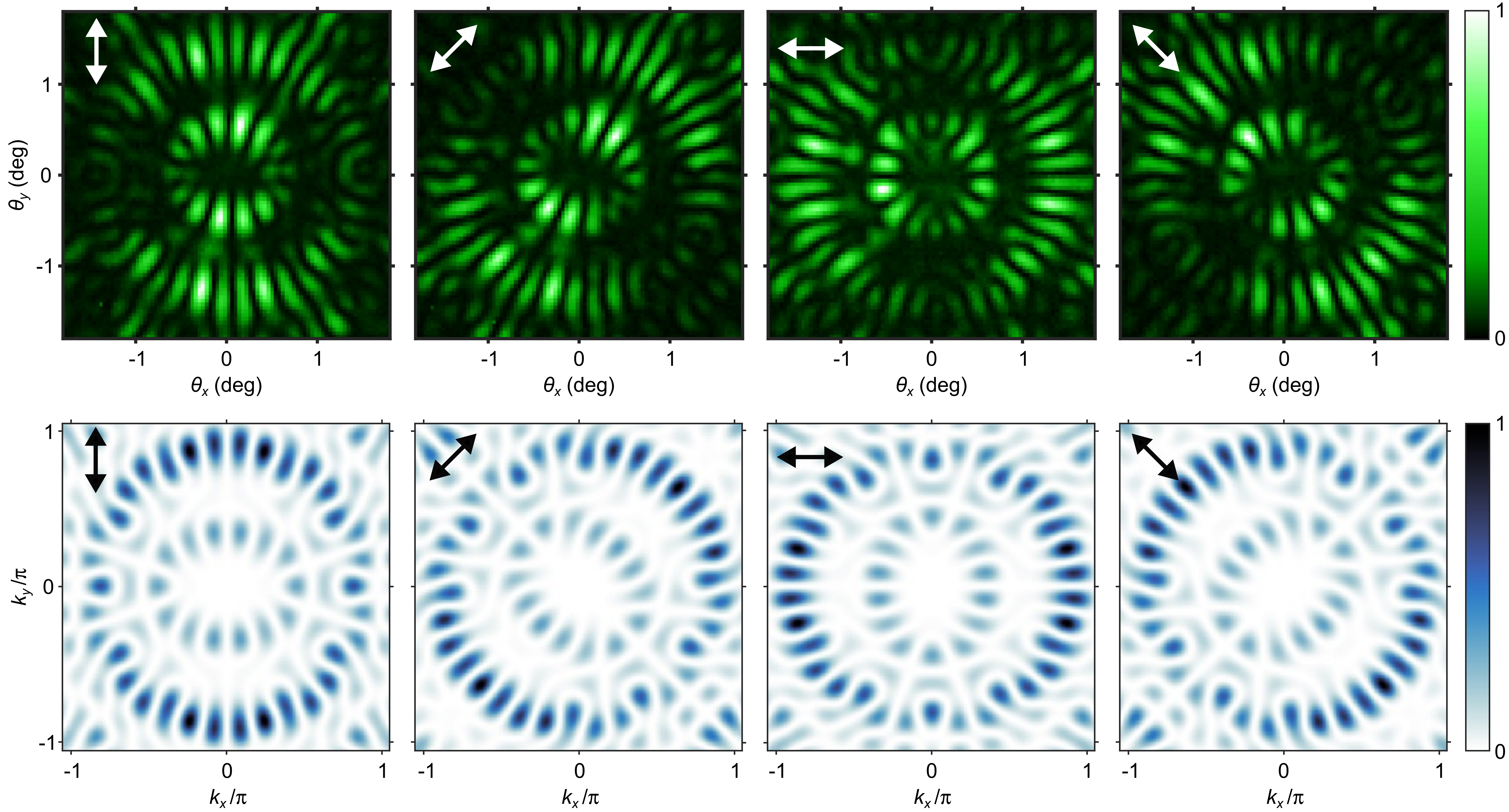

Arjas, GS et al., *Nat. Commun.* **15**, 9544 (2024)

A quasicrystal with C_{12} symmetry

Coherence and "flat-band-like" features of the lasing mode

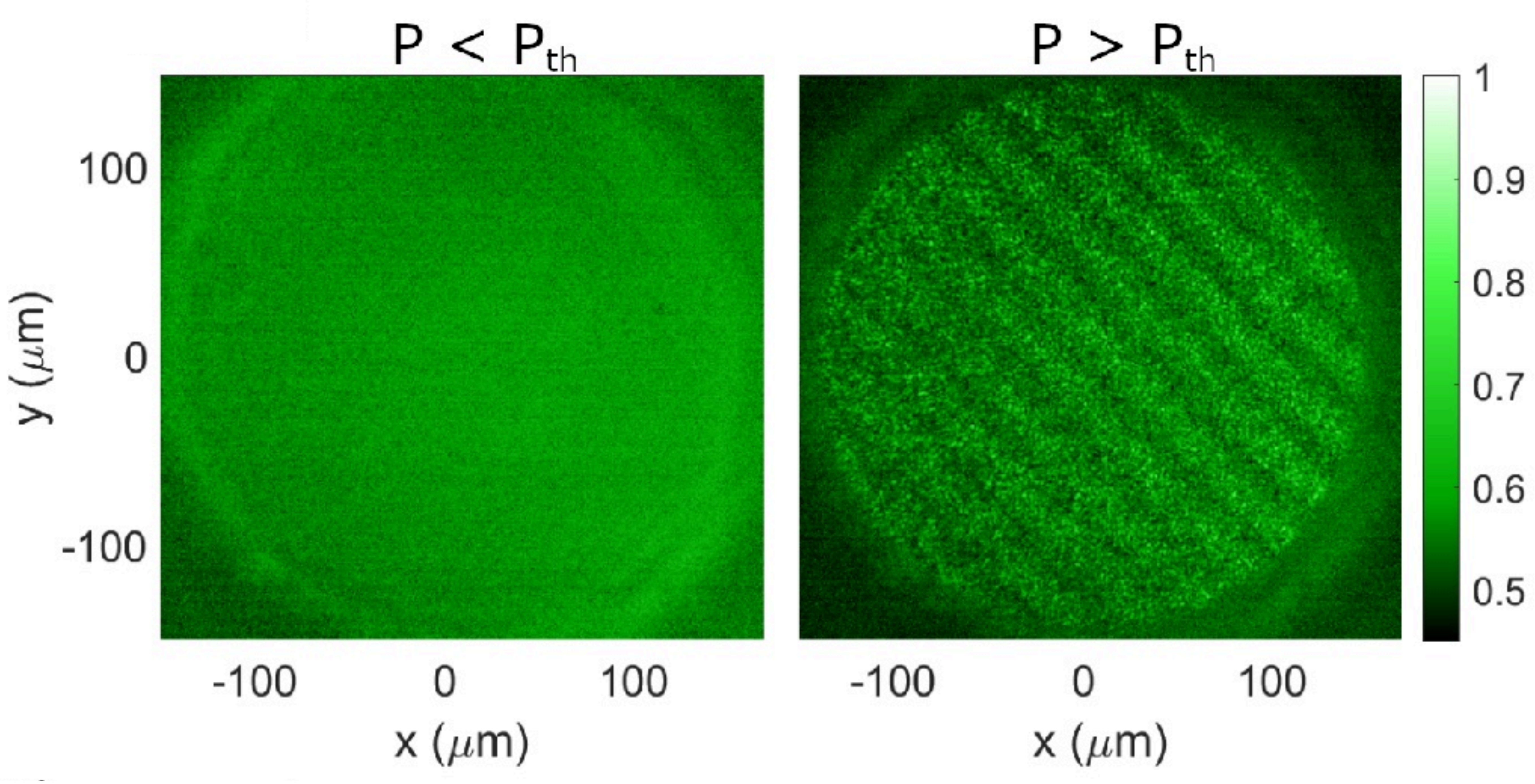

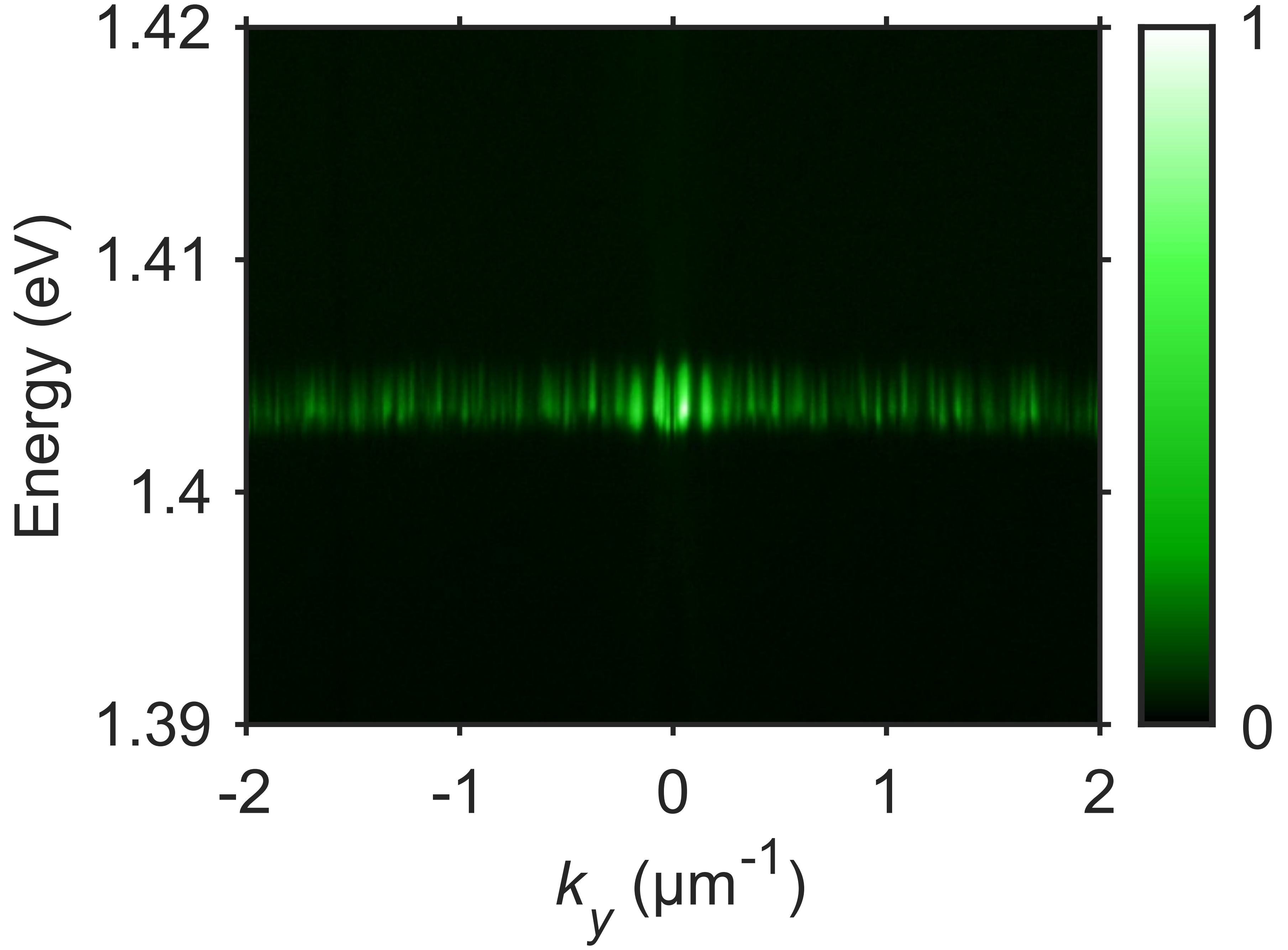

Arjas, GS et al., *Nat. Commun.* **15**, 9544 (2024)

Thanks for your attention!

- *Non-Hermitian effective model to describe BICs in photonic crystals*
- *BICs can alter the topology of the far-field*
- *Lasing in BICs from lattices with different rotational symmetries tuned by plasmonic losses*

R. Heilmann, G. Salerno, J. Cuerda, TK Hakala, and P. Törmä, *ACS Photonics* **9** 224 (2022)
G. Salerno, R. Heilmann, K. Arjas, K. Aronen, J.P. Martikainen, and P. Törmä, *Phys. Rev. Lett.* **129** 173901 (2022)
K. Arjas, J. M. Taskinen, R. Heilmann, G. Salerno and P. Törmä, *Nat. Commun.* **15**, *9544* (2024)
X. Yuan, L. Malgrey, H. Sigurðsson, H.S. Nguyen, and G. Salerno, *Phys. Rev. Research* **7**, *043141* (2025)

Grazia Salerno — Università di Pisa